

Ethionamide Boosters. 2. Combining Bioisosteric Replacement and Structure-Based Drug Design To Solve Pharmacokinetic Issues in a Series of Potent 1,2,4-Oxadiazole EthR Inhibitors[†]

Marion Flipo,^{‡,§,||,L,#,¶} Matthieu Desroses,^{‡,§,||,L,#,¶} Nathalie Lecat-Guillet,^{‡,∞,×,●,L,#} Baptiste Villemagne,^{‡,§,||,L,#} Nicolas Blondiaux,^{‡,∞,×,●,L,#,¶} Florence Leroux,^{‡,§,||,L,#} Catherine Piveteau,^{‡,§,||,L,#} Vanessa Mathys,[△] Marie-Pierre Flament,^{‡,£,#} Juergen Siepmann,^{‡,£,#} Vincent Villeret,^{‡,◇} Alexandre Wohlkönig,[⊗] René Wintjens,^{◆,◇} Sameh H. Soror,[⊗] Thierry Christophe,^{▽,†} Hee Kyoung Jeon,[▽] Camille Locht,^{‡,∞,×,●,L} Priscille Brodin,^{‡,∞,×,●,L,▽} Benoit Déprez,^{*,‡,§,||,L,#} Alain R. Baulard,^{‡,∞,×,●,L,#,¶} and Nicolas Willand^{‡,§,||,L,#,¶}

[‡]Université Lille Nord de France, F-59000 Lille, France

[§]Biostructures and Drug Discovery, INSERM U761, F-59000 Lille, France

^{||}UDSL, F-59000 Lille, France

^LIPL, F-59019 Lille, France

[#]PRIM, F-59000 Lille, France

[∞]INSERM U1019, F-59000 Lille, France

[×]CNRS UMR8204, F-59021 Lille, France

[●]Center for Infection and Immunity of Lille, F-59019 Lille, France

[◇]IRI, USR 3078 CNRS, F-59658 Villeneuve d'Ascq, France

[▽]Biology of Intracellular Pathogens, Inserm Avenir, Institut Pasteur of Korea, 463-400 Gyeonggi-do, South Korea

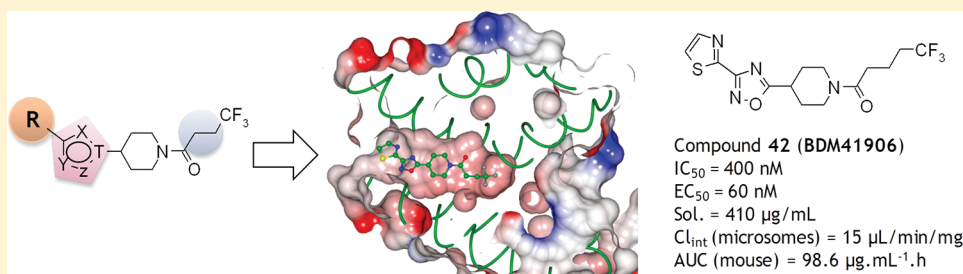
[△]Tuberculosis and Mycobacteria, Communicable and Infectious Diseases, Scientific Institute of Public Health (WIV-ISP), 1050 Brussel, Belgium

[£]INSERM U1008, F-59000 Lille, France

[⊗]Structural Biology Brussels and Molecular and Cellular Interactions, VIB, 1050 Brussel, Belgium

[◆]Laboratoire de Chimie Générale, Institut de Pharmacie, Université Libre de Bruxelles, 1050 Brussel, Belgium

S Supporting Information



ABSTRACT: Mycobacterial transcriptional repressor EthR controls the expression of EthA, the bacterial monooxygenase activating ethionamide, and is thus largely responsible for the low sensitivity of the human pathogen *Mycobacterium tuberculosis* to this antibiotic. We recently reported structure–activity relationships of a series of 1,2,4-oxadiazole EthR inhibitors leading to the discovery of potent ethionamide boosters. Despite high metabolic stability, pharmacokinetic evaluation revealed poor mice exposure; therefore, a second phase of optimization was required. Herein a structure–property relationship study is reported according to the replacement of the two aromatic heterocycles: 2-thienyl and 1,2,4-oxadiazolyl moieties. This work was done using a combination of structure-based drug design and in vitro/ex vivo evaluations of ethionamide boosters on the targeted protein EthR and on the human pathogen *Mycobacterium tuberculosis*. Thanks to this process, we identified compound 42 (BDM41906), which displays improved efficacy in addition to high exposure to mice after oral administration.

Received: June 24, 2011

Published: November 20, 2011

INTRODUCTION

By killing more than 1.8 million people per year, tuberculosis (TB) represents 2.5% of all preventable deaths globally. This makes it the leading cause of mortality resulting from a bacterial infection.¹ The major obstacles to the global control of this infectious disease include difficulties detecting and curing a sufficient number of cases to interrupt transmission.² Moreover, current estimates suggest that one-third of the world's population is infected with the latent form of the pathogen and most of the cases of TB are the result of reactivated latent infection.³ The introduction of the first-line drugs regimen to treat TB in the 1960s led to optimism that the disease could be under control. The efficacy of the drugs, coupled with increasing standards of health care, tended to rapidly decrease incidence of TB in industrialized countries, which unfortunately counteracted the effort of development of new drugs. However, since the 1980s, the global TB incidence has stopped decreasing, partly because of the co-infection with AIDS.⁴ Concomitant with this picture, one now observes the development of multidrug-resistant (MDR-TB) and extensively drug-resistant (XDR-TB) strains that more than ever strengthened the need for new drugs.⁵ However, drug-resistant tuberculosis is difficult to fight, as patients must be treated for 2–4 years with a cocktail of 4–5 second-line drugs.⁶ These drugs are often associated with serious side effects, which reduce patient compliance and thus lead to high rates of recurrence and mortality.⁷ As such, there is a concerted effort in the search for alternative molecules that are active against yet unexploited targets⁸ and for new strategies that can improve the efficacy of drugs already used in the clinic.^{9,10}

TB-DRUG BOOSTING STRATEGY

Ethionamide is a drug widely used for the treatment of MDR-TB. The efficacy of ethionamide in combination with amikacin, pyrazinamide, and moxifloxacin has been reconfirmed in mice.¹¹ As recalled by Lounis et al., this regimen is currently the most potent one against MDR-TB in this in vivo model. Consequently, as the number of MDR and XDR cases is growing worldwide, the importance of ethionamide is steadily increasing. Nevertheless, the prolonged use of ethionamide (750 mg/day for 18–24 months) generally causes serious adverse effects, such as gastrointestinal disorders, hepatitis, and various mental disturbances which may drastically reduce patient compliance and thus lead to high rates of recurrence and mortality.¹²

As with many anti-TB drugs, ethionamide is a prodrug that needs to be transformed inside the mycobacteria to show its antibacterial activity. Bioactivation of ethionamide is catalyzed by the flavin monooxygenase EthA which is under the control of the transcriptional repressor EthR, a member of the TetR family of repressors.^{13,14}

In order to improve the therapeutic index of ethionamide, we developed a new concept based on the use of EthR inhibitors that boost the bioactivation of the prodrug. In a previous work, we designed the first inhibitors and validated EthR as a druggable target. We showed that the sensitivity of *M. tuberculosis* to ethionamide can be substantially increased in vitro and in vivo by a pharmacological inhibition of EthR. Compound 1 (BDM31343, Figure 1) was able to triple the activity of ethionamide in a *M. tuberculosis* infected mice model.¹⁵ We recently reported the optimization of compound 1 by exploring the replacement of its piperidine core and cyanoacetyl group.¹⁶ EthR and 1,2,4-oxadiazole inhibitors were cocrystallized, and X-ray structures revealed the formation of a hydrogen bond

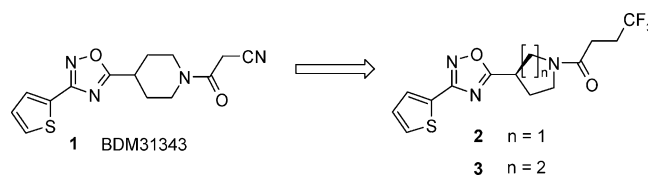


Figure 1. Structures of known EthR inhibitors.^{15,16}

between the amide function of the ligands and side chain of Asn179 located in the middle of the ligand binding domain. This work led to the discovery of two potent EthR inhibitors (compounds 2 and 3, Figure 1) that boost antibacterial activity of ethionamide in the nanomolar range. Pharmacodynamic improvements were achieved by introducing a 4,4,4-trifluorobutyl terminal chain (compound 3) and microsomal stability by replacing central 1,4-piperidyl with a (*R*)-1,3-pyrrolidyl scaffold (compound 2). In spite of this improved microsomal stability, compound 2 displayed poor mice exposure (AUC = 0.1 $\mu\text{g}\cdot\text{mL}^{-1}\cdot\text{h}$, Table 3).

To improve pharmacokinetic properties of this series while keeping high potency, we continued to explore further structure–activity and structure–property relationships by modifying the two aromatic heterocycles: 2-thienyl (compounds 4–33) and 1,2,4-oxadiazolyl rings (compounds 34–40). Structural modifications were assessed in the *N*-(4,4,4-trifluorobutyl)-piperidine series in order to avoid the stereogenic center. The efficacy of analogues was compared using previously described ex vivo phenotypic and in vitro functional assays.^{16–19} Physicochemical and pharmacokinetic properties of the most active compounds were determined in order to select a candidate for further in vivo evaluation, and cocrystallization with EthR was performed with key compound 5 to assess its binding mode. Finally, structure-based optimization of the length of the trifluoroalkyl chain led to the discovery of compound 42 (BDM41906), which presents an 8-fold increased activity profile, improved physicochemical properties, and microsomal stability, eventually leading to optimized mice exposure after oral administration (Figure 2).

CHEMISTRY

As 2-thienyl derivatives previously optimized are susceptible to forming reactive metabolites²⁰ such as epoxides or sulfoxides,^{21,22} we explored modification or replacement of the 2-thienyl ring by aromatic, heteroaromatic, or aliphatic rings (compounds 4–33). The synthesis of compounds 4–33 proceeded in four steps from commercial or synthesized carbonitriles (Scheme 1). Thiazole-2-carbonitrile and thiazole-5-carbonitrile leading to compounds 5 and 6 were synthesized in two steps from 1,3-thiazole-2-carbaldehyde and 1,3-thiazole-5-carbaldehyde, respectively.²³ Amidoximes, obtained using hydroxylamine hydrochloride, reacted with Boc-isonipecotic acid and HBTU as activating agent. The acylated products were isolated by precipitation in water prior to cyclization in DMF at 120 °C to yield the desired 1,2,4-oxadiazole ring (compounds 4b–33b).²⁴ Deprotection of the Boc-protecting group in acidic conditions was followed by acylation with 4,4,4-trifluorobutyric acid using EDCI and HOBt as coupling agents to yield compounds 4–33.

Further optimization was performed with the replacement of the 1,2,4-oxadiazole ring by isomeric or isosteric aromatic heterocycles according to the chemistry described in Scheme 2 (compounds 34–40). Thiazole derivatives (compounds 34 and 37) were obtained in three steps. Condensation of 2-bromo-1-thiophen-2-ylethanone or 2-bromoacetophenone with 4-thiocarbamoylpiperidine-1-carboxylic acid *tert*-butyl ester was achieved

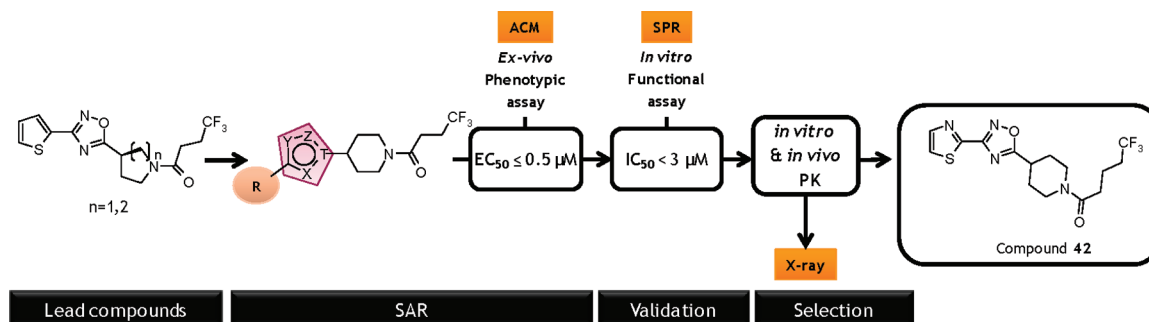
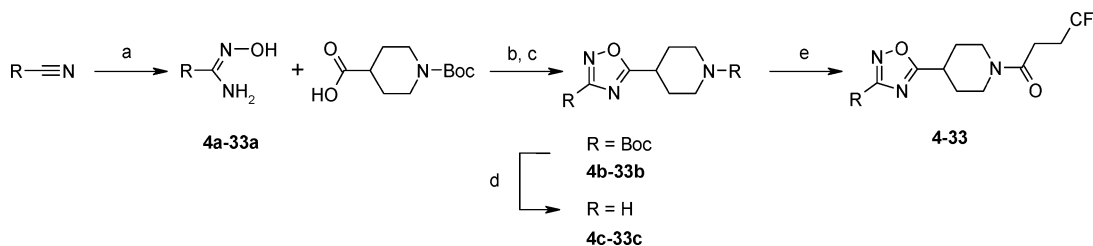


Figure 2. Optimization process of EthR inhibitors that led to the discovery of compound 42.

Scheme 1. Synthesis of 1,2,4-Oxadiazole Derivatives for SAR Studies^a



^aReagents and reaction conditions: (a) 1.5 equiv of $\text{NH}_2\text{OH}\cdot\text{HCl}$, 1.6 equiv of DIEA, EtOH, reflux; (b) 1 equiv of Boc-isonipecotic acid, 1.1 equiv of HBTU, 3 equiv of DIEA, DMF, RT, 2 h to overnight; (c) DMF, 120 °C, 4–24 h; (d) 5 equiv of 4 N HCl dioxane, RT, 4 h to overnight; (e) 1.3 equiv of 4,4,4-trifluorobutyric acid, 1.3 equiv of EDCI, 0.3 equiv of HOBT, 4 equiv of DIEA, DMF, RT, overnight.

in THF, followed by piperidine deprotection in acidic conditions and finally acylation with 4,4,4-trifluorobutyric acid using EDCI as coupling agent. The reverse 1,2,4-oxadiazole derivative (compound 35) was synthesized from 4-cyanopiperidine-1-carboxylic acid *tert*-butyl ester. The corresponding amidoxime obtained using hydroxylamine hydrochloride was acylated with thiophene-2-carboxylic acid using HBTU and then cyclized in DMF. Deprotection and acylation of piperidine yielded the desired compound. Compounds 36 and 38 were obtained in one step by acylation of commercially available 4-(5-(2-thienyl)-1*H*-pyrazol-3-yl)piperidine and 4-(5-phenyl-1,3,4-oxadiazol-2-yl)piperidine as described previously. Oxazole analogue (compound 39) was obtained by the condensation of benzaldehyde oxime with 4-ethynylpiperidine-1-carboxylic acid *tert*-butyl ester, synthesized from 4-formylpiperidine-1-carboxylic acid *tert*-butyl ester and diazo(diethoxyphosphoryl)acetic acid methyl ester as already described in the literature.²⁵ To replace 1,2,4-oxadiazole by a pyrazolone ring (compound 40), ethyl benzoylacetate and 4-hydrazinopiperidine dihydrochloride were heated in ethanol under microwave irradiation followed by free piperidine acylation with 4,4,4-trifluorobutyric acid.

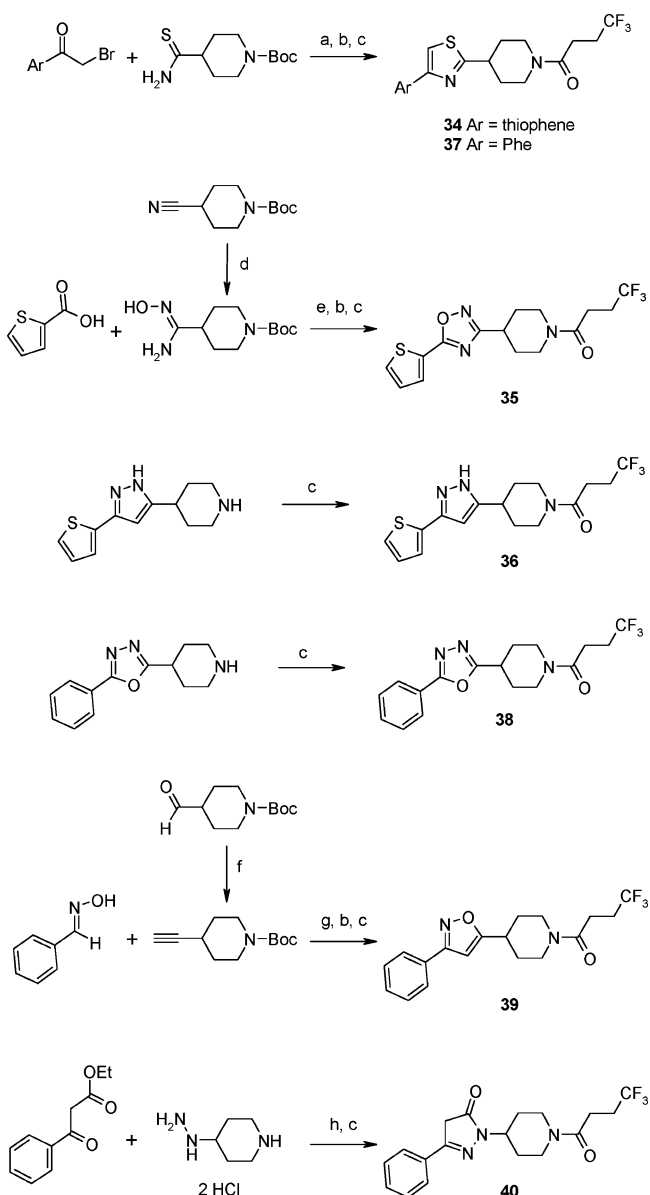
RESULTS AND DISCUSSION

In this study, we explored SAR by replacing either the thiophene (compounds 4–33) or the oxadiazole (compounds 34–40) in *N*-(4,4,4-trifluorobutyl)piperidine series. Compounds 4–40 were screened as previously described on *M. tuberculosis* infected macrophages in the presence of subactive concentration of ethionamide.¹⁶ The concentration of ligand that allows a dose of 0.1 $\mu\text{g}/\text{mL}$ ethionamide ($\text{MIC}_{99}/10$) to inhibit 50% of *M. tuberculosis* growth in macrophages was determined and expressed as EC_{50} .

First, we investigated the replacement of a 2-thienyl ring (compound 3) by five-member or six-member aromatic or aliphatic rings (Table 1). Introduction of a methylene spacer between the

two heteroaromatic rings led to a compound 10 times less active (compound 4). Introduction of a 2-thiazolyl ring (compound 5, $\text{EC}_{50} = 0.5 \mu\text{M}$) led to a slight decrease of activity. Fusion of the thiazol ring with a methoxy substituted benzene ring (compound 7, $\text{EC}_{50} = 0.2 \mu\text{M}$) restored activity. 5-Thiazolyl was less favorable (compound 6, $\text{EC}_{50} = 2.5 \mu\text{M}$), as it led to a compound 25 times less active than reference compound 3. The bioisosteric replacement of a 2-thienyl ring by phenyl slightly reduced activity (compound 8, $\text{EC}_{50} = 0.5 \mu\text{M}$). Introduction of basic six-member nitrogen rings, pyrazine (compound 9, $\text{EC}_{50} > 10 \mu\text{M}$), pyrimidine (compound 10, $\text{EC}_{50} = 9.0 \mu\text{M}$), and pyridine (compounds 11–13), strongly affected activity. Substitutions of the phenyl ring in ortho, meta, and para positions with fluorine and chlorine were also strongly detrimental for activity except compounds 15 and 19 for which activity was only slightly reduced (compound 15, $\text{EC}_{50} = 1.0 \mu\text{M}$ and compound 19, $\text{EC}_{50} = 1.1 \mu\text{M}$). Substitution with an electron-donating group such as methoxy was also detrimental for activity (compounds 23–25), whereas introduction of a methyl group was more tolerated (compounds 20–22). Substitution with large electron-withdrawing group such as trifluoromethyl group (compounds 26–28) destroyed activity except in the para position but led to a compound 5 times less active than a nonsubstituted phenyl derivative (compound 8). Hydrogen-bond donor or acceptor functions such as hydroxyl (compound 29) or dimethylamino (compound 30) introduced in the para position of the phenyl ring strongly reduced activity. The same result was obtained with a bulky *tert*-butyl group (compound 31). Replacements by five- and six-member aliphatic rings were also tested. Cyclopentyl group led to submicromolar active compound 32 ($\text{EC}_{50} = 0.8 \mu\text{M}$), whereas higher homologation strongly reduced activity (compound 33, $\text{EC}_{50} = 4.0 \mu\text{M}$).

This first structure–activity relationship study revealed the importance of 2-thienyl moiety for intracellular activities. Replacement by a nonsubstituted phenyl ring was tolerated as well as by

Scheme 2. Synthesis of Compounds 34–40^a

^aReagents and reaction conditions: (a) THF, 70 °C, overnight; (b) 4 N HCl, dioxane, RT, overnight; (c) 2 equiv of 4,4,4-trifluorobutyric acid, 2 equiv of EDCl, 4 equiv of TEA, DCM, RT, overnight; (d) 1.5 equiv of H₂NOH·HCl, 1.6 equiv of DIEA, EtOH, reflux, 5 h; (e) 1 equiv of HBTU, 2.5 equiv of DIEA, DMF, RT, overnight, then 110 °C, 5 h; (f) diazo(diethoxyphosphoryl)acetic acid methyl ester, 2 equiv of K₂CO₃, MeOH, RT, overnight; (g) NaOCl, DCM, 0 °C, then RT, overnight; (h) EtOH, microwave 50 W, 45 min.

2-thiazolyl or 6-methoxy-2-benzothiazolyl heterocycles and cyclopentyl group.

The second part of the lead optimization process explored the use of five-member heterocycles as an alternative to the 1,2,4-oxadiazole linking motif in the 2-thienyl and phenyl series (Table 2).

Replacement of oxadiazole by a 1,3-thiazole ring in both series led to poorly soluble (data not shown) and less active compounds (compounds 34 and 37). Decrease in activity was equivalent for 2-thienyl and phenyl series. Interchanging adjacent oxygen and nitrogen atoms of 1,2,4-oxadiazole ring (compound 35, EC₅₀ = 1.0 μM) slightly reduced activity, whereas exchanging 1,2,4-oxadiazole by pyrazole strongly affected activity (compound 36,

EC₅₀ > 5.0 μM). In the phenyl series, neither introduction of 1,3,4-oxadiazole (compound 38, EC₅₀ > 5 μM), isoxazole (compound 39, EC₅₀ = 4 μM), nor pyrazolone rings (compound 40, EC₅₀ > 5 μM) led to more active compounds.

In conclusion, in the 1,2,4-oxadiazole series the 2-thienyl motif may be substituted by 2-thiazolyl, 6-methoxy-2-benzothiazolyl, phenyl, or cyclopentyl. Moreover, the presence of 1,2,4-oxadiazole ring appears to be essential for activity and in particular the position of the oxygen atom in the heterocyclic ring seems critical. Only 1,3-thiazolyl motif introduction maintained submicromolar activity; however, the activity was 8 times reduced in comparison with that of the 1,2,4-oxadiazole reference compound 3. Structure–activity relationships are summarized in Figure 3.

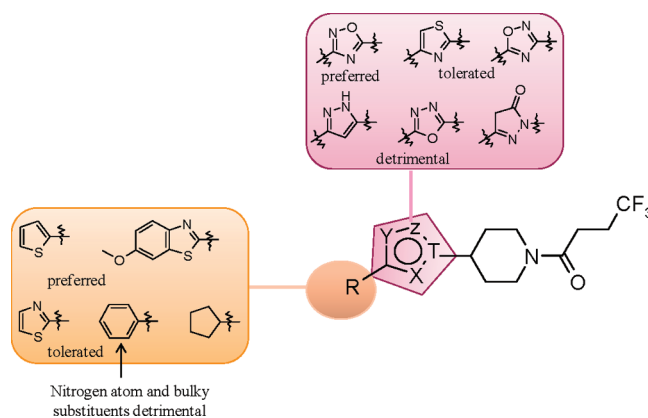


Figure 3. Summary of SAR study.

In order to confirm that the boosting activity of submicromolar compounds 5, 7, and 8 (EC₅₀ ≤ 0.5 μM) is specifically linked to the inhibition of EthR, we tested their capacity to inhibit the binding of EthR to its DNA operator, using the previously described functional surface plasmon resonance (SPR) assay.¹⁶ All tested compounds inhibited binding of EthR to its promoter in a dose dependent manner with IC₅₀ in the micromolar range (Table 3).

Compounds displaying IC₅₀ < 3 μM were further evaluated for their solubility and microsomal stability. Whereas all compounds are compliant with Lipinski and Veber's rules^{26,27} (data not shown), they present significantly different physicochemical and pharmacokinetic properties. The most lipophilic compound (compound 7, clogP = 3.22) was also the less soluble (solubility = 6 μg/mL). Conversely, the less lipophilic derivative (compound 5, clogP = 1.61) appeared to be the most soluble analogue in the 1,2,4-oxadiazole series (solubility = 300 μg/mL). As previously described, compound 3 (t_{1/2} = 5 min) was far less stable than the (R)-1,3-pyrrolidine derivative in mouse microsomes (compound 2, t_{1/2} = 298 min).¹⁶ Replacement of 2-thienyl by 2-thiazolyl enhanced microsomal stability (compound 5, t_{1/2} = 34 min, Cl_{int} = 37 μL·min⁻¹·mg⁻¹). On the basis of this observation, we decided to synthesize compound 41 which combine 2-thiazolyl and (R)-1,3-pyrrolidine as key modifications. Unfortunately, this compound was 10 times less active than the two parent compounds, which disqualified it for further ADME studies. Conversely, compound 7, which had promising activities, was unfortunately poorly soluble (6 μg/mL) and stable on microsomes (t_{1/2} = 6 min). The in vivo pharmacokinetic parameters of the most stable compounds 2 and 5 were then evaluated in mice by oral administration at 20 mg/kg using DMSO as vehicle. Area under the concentration–time curve (AUC) for

Table 1. Intracellular Activities of Compounds 3–33

Compd	R	EC ₅₀ (μ M) ^a	Compd	R	EC ₅₀ (μ M) ^a
3		0.1	19		1.1
4		1.3	20		1.2
5		0.5	21		2.3
6		2.5	22		2.2
7		0.2	23		>10.0
8		0.5	24		10.0
9		20	25		>10.0
10		9.0	26		>10.0
11		>10.0	27		>10.0
12		4.3	28		2.5
13		9.3	29		10.0
14		10.0	30		10.0
15		1.0	31		>10.0
16		7.9	32		0.8
17		6.3	33		4.0
18		10.0			

^aEC₅₀ represents the concentration of ligand that allows ethionamide at 0.1 μ g/mL (normal MIC/10) to inhibit 50% of *M. tuberculosis* growth in macrophages. EC₅₀ values are the mean of two experiments. SD was <10% in most cases.

compounds 2 and 5 were respectively 0.1 and 73.5 μ g·mL⁻¹·h (Table 3). Despite its good microsomal stability, compound 2 displays a poor in vivo exposure maybe due to low absorption after oral administration. Therefore its plasma concentration is above its EC₅₀ value (0.5 μ M) for only 30 min (see Supporting Information). At this stage, compound 5 presented the best compromise in terms of activity, solubility, microsomal stability, and mouse exposure. In order to reduce potential toxicity inherent to repeated in vivo administration of DMSO, we further evaluated

a more convenient aqueous hydroxypropyl- β -cyclodextrin-based formulation and AUC for compound 5 reached 100.5 μ g·mL⁻¹·h (Table 3). The plasma concentration of this compound was above 30 times its EC₅₀ value (0.5 μ M) for more than 4 h (see Supporting Information).

To gain insight in the interactions between compound 5 and EthR, cocrystals were produced (Figure 4). X-ray diffraction data revealed that the oxadiazole and the piperidine are facing, respectively, Trp103 and Trp207, while the 4,4,4-trifluorobutyryl

Table 2. Intracellular Activities of Compounds 3, 8, and 34–40

Compd	Ar	X	Y	Z	T	EC ₅₀ (μM) ^a
3		N	N	O	C	0.1
34		N	CH	S	C	0.8
35		N	O	N	C	1.0
36		CH	N	NH	C	>5.0
8		N	N	O	C	0.5
37		N	CH	S	C	3.2
38		O	N	N	C	>5.0
39		CH	N	O	C	4.0
40		N	CH ₂	C=O	N	> 5.0

^aEC₅₀ represents the concentration of ligand that allows ethionamide at 0.1 μg/mL (normal MIC/10) to inhibit 50% of *M. tuberculosis* growth in macrophages. EC₅₀ values are the mean of two experiments. SD was <10% in most cases.

chain points toward Trp138 and Phe184. As previously observed for other ligands, amide function is hydrogen bonded to the side chain of Asn179. Importantly, a second hydrogen bond seems to connect the oxygen atom of the 1,2,4-oxadiazole with Thr149. This observation is in agreement with our SAR study revealing that the oxygen atom in this heterocycle is crucial for activity.

This cocrystal structure also suggests that the bottom of the hydrophobic pocket of EthR may advantageously accept analogues with an extended flexible hydrophobic chain. Thus, extension of the 4,4,4-trifluorobutyl chain length by one supplementary methylene spacer (compound 42) was achieved according to Scheme 1 by coupling the free piperidine 5c with 5,5,5-trifluoropentanoic acid. Excitingly, this key modification led to a compound 8-fold more active than 5, reaching the best activities in this series with IC₅₀ and EC₅₀ equal to 400 and 60 nM, respectively. Compound 42 also proved to have the best physicochemical and pharmacokinetic properties including high solubility in PBS aqueous buffers (410 μg/mL) and fairly good stability in mouse liver microsomes with an intrinsic clearance equal to 15 μL·min⁻¹·mg⁻¹ (Table 3). Since it turned out to be one of the most promising compounds of this series, compound 42 was formulated in hydroxypropyl-β-cyclodextrin aqueous solution and administered to mice as a single oral dose of 20 mg/kg. The AUC for this compound reached a reasonable value of 98.6 μg·mL⁻¹·h, and the plasma concentration was above 30 times its EC₅₀ (0.06 μM) for more than 4 h (see Supporting Information). The crystal structure of EthR in complex with compound 42 showed a network of hydrogen bond involving

Asn179 identical to the one observed with compound 5 (Figure 5). However, the ligand has been forced to move up which abolished hydrogen bond interaction between 1,2,4-oxadiazole ring and Thr149. But the improved functional activity of compound 42 is probably due to better van der Waals interactions along the surface, especially between the trifluoroaliphatic chain and the hydrophobic bottom pocket composed of Trp145, Trp138, Phe184, and Glu180.

CONCLUSION

In this study, we have extensively explored the structure–activity and structure–property relationships of 1,2,4-oxadiazole derivatives and bioisosteric analogues as EthR inhibitors and ethionamide boosters. The challenge of this work was to improve microsomal stability and mice exposure of this series while keeping pharmacological potency. On the basis of a previous SAR study,¹⁶ we first explored replacement of a 2-thienyl heterocycle by five or six-member heteroaromatic, aromatic, or alicyclic rings. The best compromise was obtained with a bioisosteric 1,3-thiazol-2-yl ring (compound 5). This first modification did not improve activity but did enhance solubility and microsomal stability. In the second step, we demonstrated that both the nature and the position of the oxygen and nitrogen atoms of the 1,2,4-oxadiazole heterocycle are optimal to ensure efficient inhibition of EthR. Finally, exploring X-ray crystal structure of compound 5, liganded to EthR, we optimized ligand–receptor interactions by lengthening the 4,4,4-trifluorobutyl chain to a 5,5,5-trifluoropentenyl chain in order to optimize hydrophobic contacts. This modification led to the discovery of compound 42 (BDM41906) that revealed optimal physicochemical and pharmacokinetic properties and at the same time that was able to boost 10-fold ethionamide activity on *M. tuberculosis* infected macrophages at nanomolar concentration (EC₅₀ = 60 nM). Notably, this compound revealed good systemic exposure following oral administration at 20 mg/kg (AUC = 98.6 μg·mL⁻¹·h). Encouraged by pharmacodynamic and pharmacokinetic properties, we intend to evaluate compound 42 in a mouse model of *M. tuberculosis* infection. Results will be reported in due course.

EXPERIMENTAL SECTION

Biology. EthR-DNA Binding Assay. SPR analysis of the molecular interactions between EthR and the *ethA* promoter region was performed using “research grade streptavidin-coated sensor chips (sensor chip SA, Biacore Inc.)” on a BIAcore3000 instrument (Biacore, Uppsala, Sweden). The 106-bp biotinylated DNA fragment overlapping the *ethA/ethR* intergenic region was obtained by polymerase chain reaction (PCR), purified by agarose gel electrophoresis, and immobilized onto the SA sensor chip. The biotinylated DNA fragment was injected into one channel of the chip at 150 ng/mL to obtain a 75 resonance unit (RU) stable fixation to immobilize streptavidin. Another channel of the chip was loaded with a biotinylated double stranded 113-bp long irrelevant DNA fragment (+14 to +127 fragment of the *E. coli* bla gene PCR amplified using oligonucleotides O-343 (TTCCGTGTTCGCCCTTATTCC) and O-344 (CCTACTCGTG-CACCCAAGTAT) and pUC18 as substrate). Binding of EthR to the immobilized DNA was performed at 25 °C in 10 mM Tris-HCl (pH 7.5), 200 mM NaCl, 0.1 mM EDTA, 1 mM DTT, and 1% DMSO at a flow rate of 20 μL/min for 3 min. Specific interaction (SI) between EthR and the 106-bp DNA fragment was defined as the signal difference between both channels. For dose response curves establishment, the test compounds were serially diluted in the binding buffer containing 590 nM EthR, incubated for 5 min at 37 °C, and then injected in the BIAcore at a flow rate of 20 μL/min for 3 min. SI values were measured at the end of the injection period and used to

Table 3. Biological Activities, Physicochemical Properties, Mouse Microsomal Stability, and PK Parameters of Compounds 2, 3, 5, 7, 8, 41, and 42^f

Cpd	Structure		Biological activity		Physicochemical properties		Mouse microsomal stability		PK
	R	n m	EC ₅₀ (μM) ^a	IC ₅₀ (μM) ^b	clogP ^c	Solubility ^d (μg/mL)	t _{1/2} (min) ^e	CL _{int} ^f (μL/min/mg) ^e	AUC _∞ (μg·mL ⁻¹ ·h)
2		1 1	0.4	2.0	2.38	80	298	4	0.1 ^g
3		2 1	0.1	1.6	2.70	150	5	213	-
5		2 1	0.5	2.8	1.61	300	34	37	73.5 ^g 100.5 ^h
7		2 1	0.2	1.0	3.22	6	6	197	-
8		2 1	0.5	9.1	2.75	40	-	-	-
41		1 1	6.3	-	1.29	-	-	-	-
42		2 2	0.06	0.4	2.06	410	81	15	98.6 ^h

^aEC₅₀ represents the concentration of ligand that allows ethionamide at 0.1 μg/mL (normal MIC/10) to inhibit 50% of *M. tuberculosis* growth in macrophages. ^bIC₅₀ represents the concentration of ligand that inhibits 50% of the interaction of EthR with its promoter. ^cclogP was calculated using Pipeline Pilot software from Accelrys. ^dSolubilities were determined at pH 7.4. ^ePropranolol, known as a high hepatic clearance drug in rodents, was used as reference for microsomal incubations (t_{1/2} = 13 min, CL_{int} = 121 μL·min⁻¹·mg⁻¹). ^fAll the compounds have been tested in the same conditions at one concentration (1 μM). The values given here should not be read as bona fide clearance values but as indicators to rank compounds according to metabolic stability. ^gDose: 20 mg/kg. Vehicle: 100% DMSO. ^hDose: 20 mg/kg. Vehicle: aqueous solution of 100 mM hydroxypropyl-β-cyclodextrin-based formulation. ⁱSee Experimental Section for details on all assays.

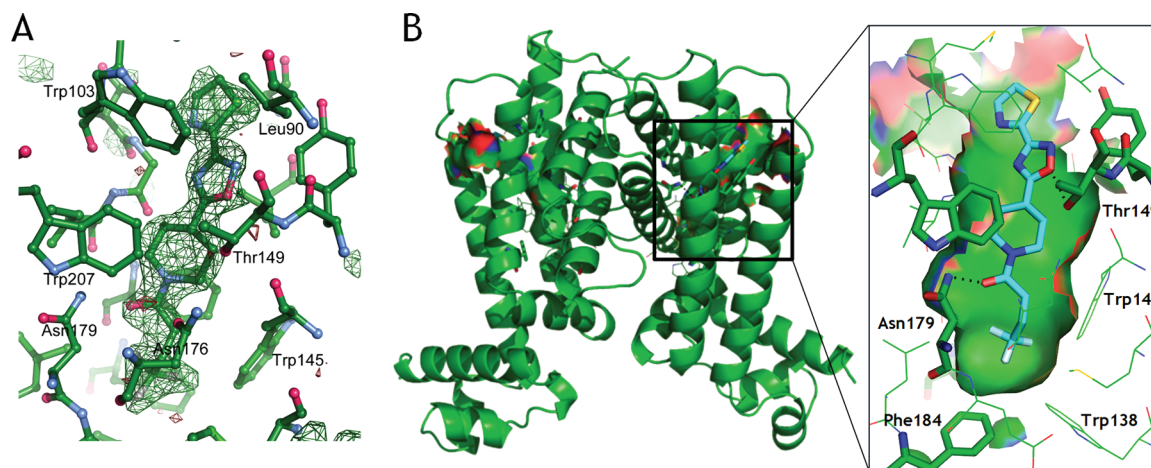


Figure 4. (A) X-ray structure representation of the ligand-binding pocket of mycobacterial transcriptional repressor EthR filled with compound 5 (PDB code 3SDG) surrounded by its omit $F_o - F_c$ map at 3.0σ contour level. The $F_o - F_c$ map was calculated prior to adding the ligand to the model. (B) X-ray structure representation of the homodimeric conformation of EthR filled in both monomers with compound 5. Surface of ligand binding domain is highlighted, and hydrogen bonds with Asn179 and Thr149 are represented with dotted line. Colors represent the following: blue (compound 5) or green (EthR) = carbon, dark blue = nitrogen, red = oxygen, yellow = sulfur, white = fluorine. Images were generated with Pymol.

calculate the inhibition of protein–DNA interaction. IC₅₀ values were determined using GraphPad Prism software.

Intracellular Assay. Raw264.7 macrophages (10⁸ cells) were infected with H37Rv-GFP suspension at a MOI of 1:1 in 300 mL for 2 h at 37 °C with shaking (100 rpm). After two washes by centrifugation at 1100 rpm for 5 min, the remaining extracellular bacilli from the infected cells suspension were killed by a 1 h Amykacin (20 μM, Sigma, A2324-5G) treatment. After a final centrifugation step, 40 μL

of *M. tuberculosis* H37Rv-GFP colonized macrophages were dispensed with the Wellmate (Matrix) into 384-well Evotec plates preplated with 10 μL of compound mixture diluted in cell medium and incubated for 5 days at 37 °C, 5% CO₂. Macrophages were then stained with SYTO 60 (Invitrogen, S11342) for 1 h followed by plate sealing. Confocal images were recorded on an automated fluorescent ultrahigh-throughput microscope, Opera (Evotec). This microscope is based on an inverted microscope architecture that allows imaging of cells cultivated

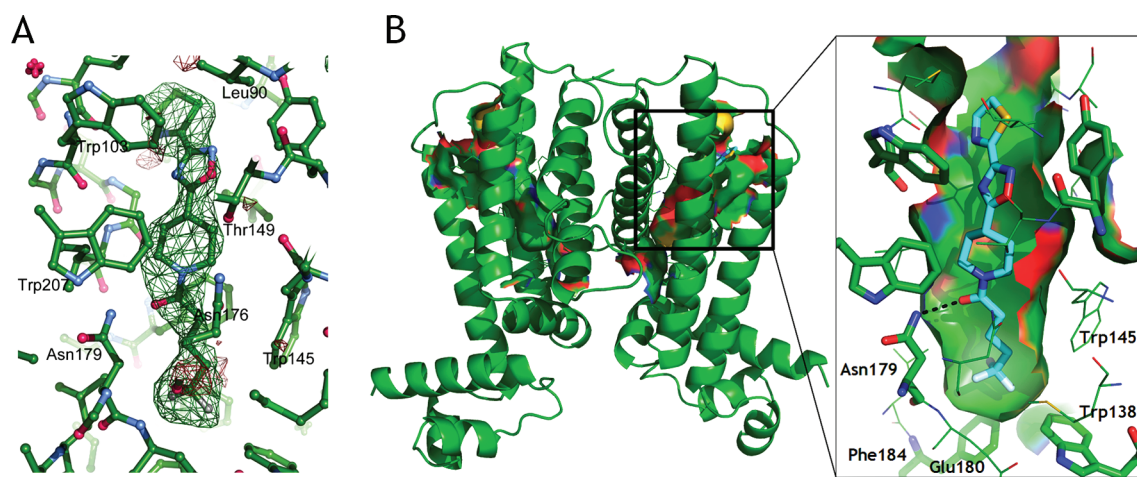


Figure 5. (A) X-ray structure representation of the ligand-binding pocket of mycobacterial transcriptional repressor EthR filled with compound **42** (PDB code 3SFI) surrounded by its initial omit $F_o - F_c$ map at 3.0σ contour level. The $F_o - F_c$ map was calculated prior to adding the ligand to the model. (B) X-ray structure representation of the homodimeric conformation of EthR filled in both monomers with compound **42**. Surface of ligand binding domain is highlighted, and the hydrogen bond with Asn179 is represented with dotted line. Colors represent the following: blue (compound **42**) or green (EthR) = carbon, dark blue = nitrogen, red = oxygen, yellow = sulfur, white = fluorine. Images were generated with Pymol.

in 96- or 384-well microplates (Evotec). Images were acquired with a $20\times$ water immersion objective (NA 0.70). A double laser excitation (488 and 635 nm) and dedicated dichroic mirrors were used to record green fluorescence of mycobacteria and red fluorescence of the macrophages on two different cameras, respectively. A series of four pictures at the center of each well were taken, and each image was then processed using dedicated image analysis.^{17,18} The percent of infected cells and the number of cells are the two parameters extracted from images analysis as previously reported.¹⁸ Data are the average of two replicates.

Potency Assay of Test Compounds on *M. tuberculosis* (Ethionamide Concentration Fixed at 0.1 $\mu\text{g}/\text{mL}$, Serial Dilution of Test Compounds). Ethionamide (Sigma E6005-5G) is diluted into DMSO to 10 mg/mL, and aliquots are stored frozen at -20°C . Test compounds are suspended in pure DMSO at 40 mg/mL in Matrix tubes and then diluted by a 10-fold dilution to 4 mg/mL in Eppendorf tubes. Ten 2-fold serial dilutions of compounds are performed in DMSO in Greiner 384-well V-shape polypropylene plates (Greiner, no. 781280). Equal volumes (5 μL) of diluted compounds and of ethionamide are transferred to a 384-well low volume polypropylene plate (Corning, no. 3672). Two independent replicates were done for each setting. On the day of the experiment, 0.5 μL of compound-plate is transferred by EVOBird platform (Evotec) to cell assay plates preplated with 10 μL of assay medium.

ADME Studies. Solubility/Metabolic Stability. These experiments were analyzed using a LC-MS-MS triple-quadrupole system (Varian 1200ws) under SIM or MRM detection with optimized mass parameters (declustering potential, collision energy, and drying gas temperature).

Solubility. The 10 mM solution (40 μL) in DMSO of the sample was added to 1.960 mL of MeOH or PBS at pH 7.4. The samples were gently shaken for 24 h at room temperature, then centrifuged for 5 min, and filtered over 0.45 μm filters. An amount equal to 20 μL of each solution was added to 180 μL of MeOH and analyzed by LC-MS. The solubility was determined by the ratio of mass signal areas PBS/MeOH.

Metabolic Stability. We purchased mouse (CD-1) liver microsomes from BD Gentest. We performed all incubations in duplicate in a shaking water bath at 37°C . The incubation mixtures contained 1 μM compound with 1% methanol used as a vehicle, mouse liver microsomes (0.6 mg of microsomal protein per mL), 5 mM MgCl_2 , 1 mM NADP, 5 mM glucose 6-phosphate, 0.4 $\text{U}\cdot\text{mL}^{-1}$ glucose 6-phosphate dehydrogenase, and 50 mM potassium phosphate buffer (pH 7.4) in a final volume of 1.5 mL. We took samples at 5, 10, 20, 30, and 40 min after microsome addition, and we stopped the reactions by

adding ice-cold acetonitrile containing 1 μM internal standard (four volumes). We centrifuged the samples for 10 min at 10000g and 4°C to pellet precipitated microsomal proteins, and we subjected the supernatant to liquid chromatography-tandem mass spectrometry (LC-MS/MS) analysis. We performed control incubations with denatured microsomes with acetonitrile containing 1 μM internal standard, and we took samples at the start of the incubation and 40 min later (to evaluate the chemical stability of the compounds in the experimental conditions). For LC-MS/MS, we used a Varian HPLC-MS/MS system 1200L triple-quadrupole mass spectrometer equipped with an electrospray ionization source. Analytes were separated in incubation mixtures by HPLC with a Luna C18, 5 μm , 50 mm \times 2.1 mm column (Phenomenex). The mobile phase solvents used were 0.1% formic acid in water (A) or 0.1% formic acid in acetonitrile (B). We applied the following mobile phase gradient: 2–98% B for 2.30 min; hold at 98% B for 1.00 min; 98–2% B for 0.10 min; 2% B hold for 1.50 min. The injection volume was 10 μL , and the flow rate was $0.6\text{ mL}\cdot\text{min}^{-1}$. We quantified each compound by converting the corresponding analyte/internal standard peak area ratios to percentage drug remaining, using the initial ratio values in control incubations as 100%. We used propranolol, known as a high hepatic clearance drug in rodents, as a quality-control compound for the microsomal incubations. Intrinsic clearance was determined based on the following equation,

$$Cl_{\text{int}} = (\text{dose}/\text{AUC})/\text{concentration of microsomes}$$

and is expressed as $\mu\text{L}\cdot\text{min}^{-1}\cdot\text{mg}^{-1}$ proteins.

Formulation. Compounds were dissolved in an aqueous hydroxypropyl- β -cyclodextrin (100 mM) solution to reach a final concentration of 3 mg/mL (upon horizontal shaking in flasks at 37°C overnight) or were dissolved in 100% DMSO to reach a final concentration of 14.5 mg/mL.

Pharmacokinetic Experiments (DMSO Formulation). Compounds were administered at 20 mg per kg body weight by oral route to Swiss mice (22–24 g) (WIV-ISP breeding). Three mice per time point were anesthetized with ketamine-xylazine and were bled at 10 min, 20 min, 30 min, 1 h, 2 h, and 4 h after administration of a single dose of ligands. Blood was collected from the brachial region on lithium heparinated tubes in order to prevent coagulation. The blood samples were centrifuged (5000g, 15 min) for plasma separation.

Pharmacokinetic Experiments (Aqueous Hydroxypropyl- β -cyclodextrin Formulation). Compounds solubilized in aqueous hydroxypropyl- β -cyclodextrin solution (100 mM) were orally administered in single dose (20 mg/kg) to CD1 female mice (25–30 g) (Charles River Laboratories). After 10 min, 20 min, 30 min, 1 h,

2 h, and 4 h, mice were anesthetized with an intraperitoneal coadministration of ketamine (80 mg/kg) and Domitor (0.8 mg/kg) and blood was sampled from the inferior vena cava. Mice were immediately sacrificed by cervical dislocation. Three mice were dosed per kinetics time point. The blood samples collected on lithium heparinated tubes in order to prevent coagulation were centrifuged (5000g, 15 min, 4 °C) for plasma separation.

Plasma Samples Preparation. Plasma samples were thawed on ice. Aliquots of 50 μ L were precipitated with 450 μ L of ice cold acetonitrile containing 2-cyclopentyl-1-[4-(3-thiophen-2-yl[1,2,4]oxadiazol-5-yl)-piperidin-1-yl]ethanone¹⁶ (1 μ M) used as internal standard. The samples were vigorously mixed with a Vortex and centrifuged at 10 000

Table 4. Optimum Mass Spectrometer Conditions and Fragmentations of Compounds 2, 5, and 42

compd	precursor ions, m/z [M + H] ⁺	predominant product ion, m/z	capillary (V)	CE (V)	drying gas (°C)
2	346.1	222.1	56	20	400
5	361.1	237.1	60	30	400
42	375.1	237.1	70	35	400

rpm at 4 °C for 10 min, and the supernatants were transferred into Matrix tubes for LC–MS–MS analysis (Table 4). Spiked standard solutions (10, 50, 100, 500, 1000, 5000, 10 000, and 50 000 nM) were prepared the same way. For LC–MS/MS analysis, we used a Varian HPLC–MS/MS system 1200L triple–quadrupole mass spectrometer equipped with an electrospray ionization source. Analytes were separated in incubation mixtures by HPLC with a Luna C18, 5 μ m, 50 mm \times 2.1 mm column (Phenomenex). The mobile phase solvents used were 0.1% formic acid in water (A) or 0.1% formic acid in acetonitrile (B). We applied the following mobile phase gradient: 2–98% B for 2.30 min; hold at 98% B for 1.00 min; 98–2% B for 0.10 min; hold at 2% B for 1.50 min. The injection volume was 10 μ L, and the flow rate was 0.6 mL·min⁻¹.

Crystal Structure Determination of EthR Ligand Complexes. EthR crystals were produced by the vapor diffusion method as described previously.²⁸ The crystallization buffer contained 1.4–1.65 M ammonium sulfate (using 0.05 M increment), 15% glycerol, and 0.1 M MES, pH 6.7. The EthR ligand complexes were prepared by mixing 1 μ L of ligand (33 mM in 100% DMSO) and 9 μ L of the purified protein (9 mg/mL) and equilibrated for 30 min at room temperature.

The X-ray diffraction data were collected on a Mar CCD Mosaic3 detector using synchrotron radiation on PX beamlines (SLS, PSI, Switzerland). EthR crystals belonged to the space group *P4₁2₁2*, with one monomer in the asymmetric unit. Data collection statistics are summarized in Table 5. Indexing was performed using iMOSFLM,²⁹

and scaling and merging were performed using the CCP4 package (Collaborative Computational Project Number 4, 1994).³⁰ Both structures were refined with the macromolecular refinement program REFMAC5. Initially ligands were fitted into the density using findligand (CCP4) and then manually positioned using Coot.³¹ The final *R* (*R*_{free}) factors are 25.1% and 27.3% for compounds 5 and 42, respectively. Both structures have been deposited with the Protein Data Bank (PDB) under the accession codes 3SDG and 3SFI.

Chemistry. General Information. NMR spectra were recorded on a Bruker DRX-300 spectrometer. Chemical shifts are in parts per million (ppm). The assignments were made using one-dimensional (1D) ¹H and ¹³C spectra and two-dimensional (2D) HSQC and COSY spectra. Mass spectra were recorded with a LC–MS–MS triple–quadrupole system (Varian 1200ws) or a LCMS (Waters Alliance Micromass ZQ 2000). LCMS analysis was performed using a C18 TSK-GEL Super ODS 2 μ m particle size column, dimensions 50 mm \times 4.6 mm. A gradient starting from 100% H₂O/0.1% formic acid and reaching 20% H₂O/80% CH₃CN/0.08% formic acid within 10 min at a flow rate of 1 mL/min was used. Preparative HPLC were performed using a Varian ProStar system using an OmniSphere 10 column C₁₈ 250 mm \times 4.14 mm Dynamax from Varian, Inc. A gradient starting from 20% CH₃CN/80% H₂O/0.1% formic acid and reaching 100% CH₃CN/0.1% formic acid at a flow rate of 80 mL/min or 20% MeOH/80% H₂O/0.1% formic acid reaching 100% MeOH/0.1% formic acid was used. Purity (%) was determined by reversed phase HPLC, using UV detection (215 nm), and all compounds showed purity greater than 95%. Melting points were determined on a Büchi B-540 apparatus and are uncorrected. All commercial reagents and solvents were used without further purification.

General Procedure for Synthesis of Amidoximes (4a, 7a, 8a, 10a, 11a, 14a–33a). Carbonitrile (1 equiv), hydroxylamine chloride (1.5 equiv), and DIEA (1.6 equiv) were mixed in absolute EtOH (1 M). The reaction mixture was refluxed until all the nitrile was consumed (TLC or LCMS control), and then the solvent was evaporated under reduced pressure. The residue was dissolved in AcOEt, washed twice with water and once with brine. The organic layer was dried over MgSO₄ and then evaporated under reduced pressure.

Synthesis of 1,3-Thiazole-2-amidoxime (5a). Hydroxylamine hydrochloride (9.03 g, 130 mmol) was added to a solution of 1,3-thiazole-2-carbaldehyde (14.71 g, 130 mmol) and pyridine (10.5 mL, 130 mmol) in DCM (100 mL). The reaction mixture was stirred overnight at room temperature and then washed twice with water. The organic layer was dried over MgSO₄ and then evaporated under reduced pressure to give 15.26 g of 1,3-thiazole-2-carbaldehyde oxime (yield 92%). 1,3-Thiazole-2-carbaldehyde oxime (15.23 g, 119 mmol, 1 equiv) was dissolved in 80 mL of dioxane, and then TEA (41.4 mL, 2.5 equiv) was added. The reaction mixture was cooled to 0 °C, and then trifluoroacetic anhydride (18.3 mL, 1.1 equiv) was added dropwise

Table 5. Data Collection Statistics

	5	42
beamline	PXIII, SLS, PSI, Switzerland	PX, SLS, PSI, Switzerland
crystal data		
Matthews coefficient, V_M (Å ³ Da ⁻¹)	2.98	2.86
solvent content (%)	58.41	56.66
unit cell data		
space group	<i>P4₁2₁2</i>	<i>P4₁2₁2</i>
<i>a</i> , <i>b</i> , <i>c</i> (Å)	121.8, 121.8, 33.61	120.76, 120.76, 33.57
α , β , γ (deg)	90, 90, 90	90, 90, 90
wavelength (Å)	1.0000	1.0000
temp (K)	100	100
resolution range (Å)	33.79–1.87 (1.97–1.87)	32.30–2.34 (2.37–2.31)
no. of unique reflections	20446 (3079)	10878 (2639)
multiplicity	7.5 (6.7)	5.5 (5.6)
completeness (%)	100 (100)	99.6 (99.7)
$\langle I/\sigma(I) \rangle$	14 (3.0)	7.8 (2.3)
<i>R</i> _{merge}	9.0 (56.4)	15.8 (75.6)

to the mixture. The solution was stirred overnight at room temperature and then evaporated. The residue was dissolved in DCM and then washed twice with water. The organic layer was dried over MgSO_4 and then evaporated under reduced pressure to give 1,3-thiazole-2-carbonitrile. This compound was used in the next step without further purification. 1,3-Thiazole-2-carbonitrile (13.11 g, 119 mmol, 1 equiv), hydroxylamine hydrochloride (12.4 g, 1.5 equiv), and DIEA (33 mL, 1.6 equiv) were mixed in absolute EtOH (150 mL). The reaction mixture was refluxed 4 h, and then the solvent was evaporated under reduced pressure. The residue was dissolved in AcOEt, washed twice with water and once with brine. The organic layer was dried over MgSO_4 and then evaporated under reduced pressure to give 15.86 g of 1,3-thiazole-2-amidoxime (yield, 93% over two steps).

Synthesis of 1,3-Thiazole-5-amidoxime (6a). Hydroxylamine hydrochloride (3.07 g, 44 mmol) was added to a solution of 1,3-thiazole-5-carbaldehyde (5 g, 44 mmol) and pyridine (3.7 mL) in DCM (25 mL). The reaction mixture was stirred overnight at room temperature and then washed once with water. The product was recovered by filtration to give 5.23 g of 1,3-thiazole-5-carbaldehyde oxime (yield 92%). 1,3-Thiazole-5-carbaldehyde oxime (2.5 g, 19.5 mmol, 1 equiv) was dissolved in 12 mL of dioxane, and then TEA (6.8 mL, 2.5 equiv) was added. The reaction mixture was cooled to 0 °C, and then trifluoroacetic anhydride (3.0 mL, 1.1 equiv) was added dropwise to the reaction. The solution was stirred overnight at room temperature and then 1.1 equiv of trifluoroacetic anhydride was added to complete the reaction. The solution was stirred overnight at room temperature and then evaporated. The residue was dissolved in DCM and then washed five times with water. The organic layer was dried over MgSO_4 and then evaporated under reduced pressure to give 1.25 g of 1,3-thiazole-5-carbonitrile (yield, 58%). 1,3-Thiazole-5-carbonitrile (1 g, 9.08 mmol, 1 equiv), hydroxylamine hydrochloride (0.95 g, 1.5 equiv), and DIEA (2.5 mL, 1.6 equiv) were mixed in absolute EtOH (30 mL). The reaction mixture was refluxed for 5 h, and then the solvent was evaporated under reduced pressure. The residue was dissolved in AcOEt, washed twice with water and once with brine. The organic layer was dried over MgSO_4 and then evaporated under reduced pressure to give 940 mg of 1,3-thiazole-5-amidoxime (yield, 72%).

General Procedure for Synthesis of 1,2,4-Oxadiazole (4b–8b, 10b, 11b, 14b–33b). 1-Boc-piperidine-4-carboxylic acid (10 mmol, 1 equiv), HBTU (1.1 equiv), and DIEA (3 equiv) were dissolved in DMF (15 mL). The solution was stirred for 5 min, and then the amidoxime (4a–8a, 10a, 11a, 14a–33a) (1 equiv) was added. The reaction mixture was stirred at room temperature for 2 h to overnight and then poured in 50 mL of water. The reaction mixture became a thick crystalline slurry. The product was recovered by filtration and washed with water. Compounds 4b, 6b, and 29b did not precipitate in water. The product was extracted 3 times with AcOEt, and then the organic layers were joined, washed twice with saturated aqueous NaHCO_3 and once with brine, then dried over MgSO_4 and evaporated under reduced pressure. The solid obtained was dissolved in DMF (15 mL), and then the reaction mixture was heated at 120 °C for 4–24 h. The solvent was removed under vacuum, and the residue was dissolved in AcOEt. The organic layer was washed twice with 1 N HCl, twice with saturated aqueous NaHCO_3 , and once with brine, then dried over MgSO_4 and evaporated under reduced pressure.

General Procedure for Deprotection Step (4c–8c, 10c, 11c, 14c–33c). Boc intermediates (4b–8b, 10b, 11b, 14b–33b) were dissolved in dioxane (1 M), and 4 N HCl solution in dioxane (5 equiv) was added. The reaction mixture was stirred at room temperature for 4 h to overnight. The product was recovered by filtration and then washed with petroleum ether.

Compounds 4c, 32c and 33c did not precipitate. The dioxane was removed under reduced pressure, and then the residue was dissolved in water and washed twice with AcOEt. The pH of the aqueous phase was adjusted to 10 with saturated aqueous K_2CO_3 , and then the product was extracted 3 times with AcOEt. The organic phases were joined, washed once with brine, then dried over MgSO_4 and evaporated under reduced pressure.

Compounds 9c, 12c and 13c were purchased from Peakdale.

4-[3-Thiophen-2-ylmethyl[1,2,4]oxadiazol-5-yl]piperidine (4c). $^1\text{H NMR}$ (CDCl_3) δ 7.19 (dd, $J = 5.0$ Hz, $J = 1.4$ Hz, 1H), 6.92–6.97 (m, 2H), 4.25 (s, 2H), 3.19–3.26 (m, 2H), 3.06–3.15 (m, 1H), 2.79–2.88 (m, 2H), 2.11–2.17 (m, 2H), 1.86–1.98 (m, 2H). MS $[\text{M} + \text{H}]^+ m/z$ 250.

4-(3-Thiazol-2-yl[1,2,4]oxadiazol-5-yl)piperidine Hydrochloride (5c). White powder. $^1\text{H NMR}$ (D_2O) δ 7.96 (d, $J = 3.2$ Hz, 1H), 7.81 (d, $J = 3.2$ Hz, 1H), 3.45–3.53 (m, 3H), 3.11–3.20 (m, 2H), 2.34–2.40 (m, 2H), 2.00–2.14 (m, 2H). MS $[\text{M} + \text{H}]^+ m/z$ 237.

4-(3-Thiazol-5-yl[1,2,4]oxadiazol-5-yl)piperidine Hydrochloride (6c). White powder. $^1\text{H NMR}$ ($\text{DMSO}-d_6$) δ 9.30 (s, 1H), 8.52 (s, 1H), 3.44–3.53 (m, 1H), 3.31–3.36 (m, 2H), 3.00–3.10 (m, 2H), 2.23–2.29 (m, 2H), 1.91–2.05 (m, 2H). MS $[\text{M} + \text{H}]^+ m/z$ 237.

4-[3-(6-Methoxybenzothiazol-2-yl)-1,2,4-oxadiazol-5-yl]piperidine Hydrochloride (7c). White powder. $^1\text{H NMR}$ (D_2O) δ 7.57 (d, $J = 9.0$ Hz, 1H), 7.06 (s, 1H), 6.82 (d, $J = 9.0$ Hz, 1H), 3.67 (s, 3H), 3.50–3.70 (m, 3H), 3.24–3.31 (m, 2H), 2.43–2.48 (m, 2H), 2.08–2.20 (m, 2H). MS $[\text{M} + \text{H}]^+ m/z$ 317.

4-(3-Phenyl[1,2,4]oxadiazol-5-yl)piperidine Hydrochloride (8c). White powder. $^1\text{H NMR}$ (MeOD) δ 8.02 (m, 2H), 7.46 (m, 3H), 3.48 (m, 3H), 3.17 (m, 2H), 2.39 (m, 2H), 2.10 (m, 2H). MS $[\text{M} + \text{H}]^+ m/z$ 230.

4-(3-Pyrimidin-2-yl-1,2,4-oxadiazol-5-yl)piperidine Hydrochloride (10c). White powder. $^1\text{H NMR}$ ($\text{DMSO}-d_6$) δ 9.42–9.61 (m, 2H), 9.04 (d, $J = 4.8$ Hz, 2H), 7.73 (t, $J = 4.8$ Hz, 1H), 3.52–3.61 (m, 1H), 3.30–3.34 (m, 2H), 3.01–3.13 (m, 2H), 2.25–2.30 (m, 2H), 2.02–2.16 (m, 2H). MS $[\text{M} + \text{H}]^+ m/z$ 232.

2-(5-Piperidin-4-yl[1,2,4]oxadiazol-3-yl)pyridine Hydrochloride (11c). White powder. $^1\text{H NMR}$ (MeOD) δ 8.93 (m, 1H), 8.68 (m, 2H), 8.19 (m, 1H), 3.64 (m, 1H), 3.52 (m, 2H), 3.24 (m, 2H), 2.47 (m, 2H), 2.21 (m, 2H). MS $[\text{M} + \text{H}]^+ m/z$ 231.

4-[3-(2-Fluorophenyl)[1,2,4]oxadiazol-5-yl]piperidine Hydrochloride (14c). White powder. $^1\text{H NMR}$ ($\text{DMSO}-d_6$) δ 9.28 (brs, 2H), 8.01 (td, $J = 7.5$ Hz, $J = 1.7$ Hz, 1H), 7.62–7.69 (m, 1H), 7.38–7.47 (m, 2H), 3.49–3.59 (m, 1H), 3.30–3.36 (m, 2H), 3.02–3.11 (m, 2H), 2.23–2.29 (m, 2H), 1.99–2.12 (m, 2H). MS $[\text{M} + \text{H}]^+ m/z$ 248.

4-[3-(3-Fluorophenyl)[1,2,4]oxadiazol-5-yl]piperidine Hydrochloride (15c). White powder. $^1\text{H NMR}$ ($\text{DMSO}-d_6$) δ 9.28 (brs, 1H), 9.15 (brs, 1H), 7.85 (dt, $J = 7.8$ Hz, $J = 1.1$ Hz, 1H), 7.71–7.76 (m, 1H), 7.60–7.67 (m, 1H), 7.46 (td, $J = 8.6$ Hz, $J = 2.7$ Hz, 1H), 3.48–3.57 (m, 1H), 3.31–3.39 (m, 2H), 3.01–3.12 (m, 2H), 2.23–2.29 (m, 2H), 1.98–2.12 (m, 2H). MS $[\text{M} + \text{H}]^+ m/z$ 248.

4-[3-(4-Fluorophenyl)[1,2,4]oxadiazol-5-yl]piperidine Hydrochloride (16c). White powder. $^1\text{H NMR}$ ($\text{DMSO}-d_6$) δ 9.32 (brs, 2H), 8.05 (dd, $J = 5.5$ Hz, $J = 8.9$ Hz, 2H), 7.40 (dd, $J = 8.8$ Hz, $J = 8.9$ Hz, 2H), 3.51 (m, 1H), 3.31 (m, 2H), 3.05 (m, 2H), 2.25 (m, 2H), 2.05 (m, 2H). MS $[\text{M} + \text{H}]^+ m/z$ 248.

4-[3-(2-Chlorophenyl)[1,2,4]oxadiazol-5-yl]piperidine Hydrochloride (17c). White powder. $^1\text{H NMR}$ ($\text{DMSO}-d_6$) δ 9.33 (brs, 1H), 9.21 (brs, 1H), 7.90 (dd, $J = 7.6$ Hz, $J = 1.8$ Hz, 1H), 7.68 (dd, $J = 7.6$ Hz, $J = 1.6$ Hz, 1H), 7.61 (td, $J = 7.6$ Hz, $J = 1.8$ Hz, 1H), 7.53 (td, $J = 7.6$ Hz, $J = 1.6$ Hz, 1H), 3.55 (m, 1H), 3.32 (m, 2H), 3.06 (m, 2H), 2.27 (m, 2H), 2.05 (m, 2H). MS $[\text{M} + \text{H}]^+ m/z$ 264.

4-[3-(3-Chlorophenyl)[1,2,4]oxadiazol-5-yl]piperidine Hydrochloride (18c). White powder. $^1\text{H NMR}$ ($\text{DMSO}-d_6$) δ 9.33 (brs, 1H), 9.21 (brs, 1H), 7.95–7.98 (m, 2H), 7.68 (dt, $J = 8.0$ Hz, $J = 1.8$ Hz, 1H), 7.60 (t, $J = 8.0$ Hz, 1H), 3.48–3.58 (m, 1H), 3.30–3.38 (m, 2H), 3.01–3.12 (m, 2H), 2.23–2.29 (m, 2H), 1.99–2.12 (m, 2H). MS $[\text{M} + \text{H}]^+ m/z$ 264.

4-[3-(4-Chlorophenyl)[1,2,4]oxadiazol-5-yl]piperidine Hydrochloride (19c). White powder. $^1\text{H NMR}$ ($\text{DMSO}-d_6$) δ 9.32 (brs, 1H), 9.22 (brs, 1H), 8.01 (d, $J = 8.7$ Hz, 2H), 7.64 (d, $J = 8.7$ Hz, 2H), 3.47–3.57 (m, 1H), 3.30–3.34 (m, 2H), 3.01–3.11 (m, 2H), 2.23–2.28 (m, 2H), 1.98–2.12 (m, 2H). MS $[\text{M} + \text{H}]^+ m/z$ 264.

4-[3-(2-Methylphenyl)[1,2,4]oxadiazol-5-yl]piperidine Hydrochloride (20c). Beige powder. $^1\text{H NMR}$ ($\text{DMSO}-d_6$) δ 9.40 (brs, 1H), 9.27 (brs, 1H), 7.90 (d, $J = 7.6$ Hz, 1H), 7.34–7.49 (m, 3H), 3.47–3.57 (m, 1H), 3.30–3.39 (m, 2H), 3.01–3.11 (m, 2H),

2.54 (s, 3H), 2.23–2.29 (m, 2H), 1.99–2.13 (m, 2H). MS $[M + H]^+$ m/z 244.

4-[3-(3-Methylphenyl)[1,2,4]oxadiazol-5-yl]piperidine Hydrochloride (21c). White powder. ^1H NMR (DMSO- d_6) δ 9.34 (brs, 1H), 9.24 (brs, 1H), 7.78–7.81 (m, 2H), 7.38–7.47 (m, 2H), 3.43–3.56 (m, 1H), 3.30–3.34 (m, 2H), 3.00–3.11 (m, 2H), 2.39 (s, 3H), 2.23–2.28 (m, 2H), 1.98–2.12 (m, 2H). MS $[M + H]^+$ m/z 244.

4-[3-(4-Methylphenyl)[1,2,4]oxadiazol-5-yl]piperidine Hydrochloride (22c). White powder. ^1H NMR (DMSO- d_6) δ 9.23 (brs, 2H), 7.89 (d, $J = 8.1$ Hz, 2H), 7.37 (d, $J = 8.1$ Hz, 2H), 3.45–3.55 (m, 1H), 3.30–3.35 (m, 2H), 3.01–3.10 (m, 2H), 2.38 (s, 3H), 2.22–2.28 (m, 2H), 1.97–2.11 (m, 2H). MS $[M + H]^+$ m/z 244.

4-[3-(2-Methoxyphenyl)[1,2,4]oxadiazol-5-yl]piperidine Hydrochloride (23c). White powder. ^1H NMR (DMSO- d_6) δ 9.25 (brs, 2H), 7.82 (dd, $J = 7.5$ Hz, $J = 1.6$ Hz, 1H), 7.55 (ddd, $J = 7.5$ Hz, $J = 8.2$ Hz, $J = 1.6$ Hz, 1H), 7.22 (dd, $J = 8.2$ Hz, $J = 1.0$ Hz, 1H), 7.10 (td, $J = 7.5$ Hz, $J = 1.0$ Hz, 1H), 3.86 (s, 3H), 3.49 (m, 1H), 3.31 (m, 2H), 3.05 (m, 2H), 2.24 (m, 2H), 2.03 (m, 2H). MS $[M + H]^+$ m/z 260.

4-[3-(3-Methoxyphenyl)[1,2,4]oxadiazol-5-yl]piperidine Hydrochloride (24c). White powder. ^1H NMR (DMSO- d_6) δ 9.22 (brs, 2H), 7.58 (dt, $J = 7.7$ Hz, $J = 1.2$ Hz, 1H), 7.46–7.51 (m, 2H), 7.17 (ddd, $J = 8.2$ Hz, $J = 2.6$ Hz, $J = 1.0$ Hz, 1H), 3.83 (s, 3H), 3.46–3.56 (m, 1H), 3.31–3.35 (m, 2H), 3.01–3.09 (m, 2H), 2.23–2.29 (m, 2H), 1.98–2.11 (m, 2H). MS $[M + H]^+$ m/z 260.

4-[3-(4-Methoxyphenyl)[1,2,4]oxadiazol-5-yl]piperidine Hydrochloride (25c). White powder. ^1H NMR (DMSO- d_6) δ 9.29 (brs, 1H), 9.15 (brs, 1H), 7.93 (d, $J = 8.8$ Hz, 2H), 7.10 (d, $J = 8.8$ Hz, 2H), 3.83 (s, 3H), 3.53–3.56 (m, 1H), 3.30–3.34 (m, 2H), 3.01–3.10 (m, 2H), 2.22–2.27 (m, 2H), 1.96–2.10 (m, 2H). MS $[M + H]^+$ m/z 260.

4-[3-(2-Trifluoromethylphenyl)[1,2,4]oxadiazol-5-yl]piperidine Hydrochloride (26c). White powder. ^1H NMR (DMSO- d_6) δ 9.27 (brs, 1H), 9.10 (brs, 1H), 7.95–7.99 (m, 1H), 7.80–7.88 (m, 3H), 3.52–3.61 (m, 1H), 3.29–3.35 (m, 2H), 3.01–3.12 (m, 2H), 2.23–2.29 (m, 2H), 1.96–2.09 (m, 2H). MS $[M + H]^+$ m/z 298.

4-[3-(3-Trifluoromethylphenyl)[1,2,4]oxadiazol-5-yl]piperidine Hydrochloride (27c). White powder. ^1H NMR (DMSO- d_6) δ 9.34 (brs, 1H), 9.22 (brs, 1H), 8.30 (d, $J = 7.9$ Hz, 1H), 8.21 (s, 1H), 7.99 (d, $J = 7.9$ Hz, 1H), 7.83 (t, $J = 7.9$ Hz, 1H), 3.55 (m, 1H), 3.32 (m, 2H), 3.06 (m, 2H), 2.27 (m, 2H), 2.07 (m, 2H). MS $[M + H]^+$ m/z 298.

4-[3-(4-Trifluoromethylphenyl)[1,2,4]oxadiazol-5-yl]piperidine Hydrochloride (28c). White powder. ^1H NMR (DMSO- d_6) δ 9.37 (brs, 2H), 8.21 (d, $J = 8.5$ Hz, 2H), 7.94 (d, $J = 8.5$ Hz, 2H), 3.55 (m, 1H), 3.31 (m, 2H), 3.07 (m, 2H), 2.27 (m, 2H), 2.07 (m, 2H). MS $[M + H]^+$ m/z 298.

4-[3-(4-Hydroxyphenyl)[1,2,4]oxadiazol-5-yl]piperidine Hydrochloride (29c). Beige powder. ^1H NMR (DMSO- d_6) δ 9.17 (brs, 2H), 7.81 (d, $J = 8.7$ Hz, 2H), 6.93 (d, $J = 8.7$ Hz, 2H), 3.42–3.51 (m, 1H), 3.29–3.33 (m, 2H), 3.01–3.08 (m, 2H), 2.21–2.25 (m, 2H), 1.97–2.07 (m, 2H). MS $[M + H]^+$ m/z 246.

4-[3-(4-Dimethylaminophenyl)[1,2,4]oxadiazol-5-yl]piperidine Hydrochloride (30c). Beige powder. ^1H NMR (DMSO- d_6) δ 9.45 (brs, 1H), 9.33 (brs, 1H), 7.84 (d, $J = 8.8$ Hz, 2H), 7.00 (d, $J = 8.8$ Hz, 2H), 3.42–3.50 (m, 1H), 3.28–3.32 (m, 2H), 3.01–3.09 (m, 2H), 3.01 (s, 6H), 2.21–2.26 (m, 2H), 1.98–2.11 (m, 2H). MS $[M + H]^+$ m/z 273.

4-[3-(4-tert-Butylphenyl)[1,2,4]oxadiazol-5-yl]piperidine Hydrochloride (31c). Beige powder. ^1H NMR (DMSO- d_6) δ 9.25 (brs, 2H), 7.92 (d, $J = 8.5$ Hz, 2H), 7.58 (d, $J = 8.5$ Hz, 2H), 3.50 (m, 1H), 3.36 (m, 2H), 3.08 (m, 2H), 2.26 (m, 2H), 1.99 (m, 2H), 1.31 (s, 9H). MS $[M + H]^+$ m/z 286.

4-(3-Cyclopentyl[1,2,4]oxadiazol-5-yl)piperidine (32c). Yellow oil; ^1H NMR (DMSO- d_6) δ 2.89–3.19 (m, 4H), 2.55–2.73 (m, 2H), 1.89–2.01 (m, 4H), 1.53–1.76 (m, 8H). MS $[M + H]^+$ m/z 222.

4-(3-Cyclohexyl[1,2,4]oxadiazol-5-yl)piperidine (33c). Yellow oil; ^1H NMR (DMSO- d_6) δ 3.11–3.53 (m, 3H), 2.70–2.98 (m, 3H), 1.90–2.07 (m, 4H), 1.63–1.78 (m, 5H), 1.16–1.52 (m, 5H). MS $[M + H]^+$ m/z 236.

General Procedure for Coupling (4–33). 4,4,4-Trifluorobutyric acid (1.3 equiv), EDCI (1.3 equiv), HOBt (0.3 equiv), and DIEA (4 equiv) were mixed in DMF (2 mL) for 5 min. Piperidine intermediate (0.8 mmol, 1 equiv) was added with 3 mL of DMF. The reaction mixture was stirred overnight at room temperature and then evaporated under reduced pressure and purified by preparative HPLC.

4,4,4-Trifluoro-1-[4-(3-thiophen-2-ylmethyl-1,2,4-oxadiazol-5-yl)piperidin-1-yl]butan-1-one (4). Colorless oil. Yield 46%. ^1H NMR (CDCl₃) δ 7.19 (dd, $J = 4.9$ Hz, $J = 1.5$ Hz, 1H), 6.92–6.97 (m, 2H), 4.41–4.46 (m, 1H), 4.25 (s, 2H), 3.83–3.87 (m, 1H), 3.14–3.25 (m, 2H), 2.92–2.99 (m, 1H), 2.41–2.60 (m, 4H), 2.08–2.18 (m, 2H), 1.84–1.96 (m, 2H). ^{13}C NMR (CDCl₃) δ 180.91, 168.75, 168.08, 136.78, 127.05 (q, $J = 275$ Hz), 127.04, 126.72, 125.02, 44.37, 40.97, 34.18, 29.56 (q, $J = 29$ Hz), 29.35, 28.78, 26.72, 25.89. $t_{\text{RLCMS}} = 5.9$ min. Purity 99%. MS $[M + H]^+$ m/z 374.

4,4,4-Trifluoro-1-[4-(3-thiazol-2-yl-1,2,4-oxadiazol-5-yl)piperidin-1-yl]butan-1-one (5). White powder. Yield 55%. ^1H NMR (CDCl₃) δ 8.07 (d, $J = 3.3$ Hz, 1H), 7.60 (d, $J = 3.3$ Hz, 1H), 4.49–4.54 (m, 1H), 3.91–3.96 (m, 1H), 3.27–3.38 (m, 2H), 2.98–3.07 (m, 1H), 2.50–2.64 (m, 4H), 2.11–2.28 (m, 2H), 1.87–2.09 (m, 2H). ^{13}C NMR (CDCl₃) δ 181.78, 168.10, 164.03, 153.75, 145.01, 127.04 (q, $J = 275$ Hz), 122.56, 44.39, 40.99, 34.30, 29.59 (q, $J = 30$ Hz), 29.33, 28.80, 25.93 (q, $J = 2.8$ Hz). $t_{\text{RLCMS}} = 4.8$ min. Purity >99%. MS $[M + H]^+$ m/z 361. HRMS calcd for C₁₄H₁₅F₃N₄O₂S $[M + H]^+$, 361.0946; found, 361.0931.

4,4,4-Trifluoro-1-[4-(3-thiazol-5-yl-1,2,4-oxadiazol-5-yl)piperidin-1-yl]butan-1-one (6). White powder. Yield 61%. ^1H NMR (CD₂Cl₂) δ 8.98 (d, $J = 0.6$ Hz, 1H), 8.54 (d, $J = 0.6$ Hz, 1H), 4.50–4.55 (m, 1H), 3.91–3.96 (m, 1H), 3.25–3.37 (m, 2H), 2.94–3.03 (m, 1H), 2.46–2.67 (m, 4H), 2.17–2.26 (m, 2H), 1.81–2.02 (m, 2H). ^{13}C NMR (CD₂Cl₂) δ 181.55, 167.81, 162.71, 155.81, 145.24, 127.35 (q, $J = 275$ Hz), 124.02, 44.31, 40.85, 34.28, 29.43 (q, $J = 29$ Hz), 29.36, 28.82, 25.78. $t_{\text{RLCMS}} = 5.1$ min. Purity >99%. MS $[M + H]^+$ m/z 361.

4,4,4-Trifluoro-1-[4-(3-(6-methoxybenzothiazol-2-yl)-1,2,4-oxadiazol-5-yl)piperidin-1-yl]butan-1-one (7). White powder. Yield 47%. ^1H NMR (CDCl₃) δ 8.13 (d, $J = 9.0$ Hz, 1H), 7.40 (d, $J = 2.4$ Hz, 1H), 7.17 (dd, $J = 9.0$ Hz, $J = 2.4$ Hz, 1H), 4.52–4.57 (m, 1H), 3.93–4.00 (m, 1H), 3.93 (s, 3H), 3.25–3.40 (m, 2H), 2.97–3.05 (m, 1H), 2.45–2.65 (m, 4H), 2.19–2.28 (m, 2H), 1.94–2.07 (m, 2H). ^{13}C NMR (CDCl₃) δ 181.96, 168.11, 164.57, 159.22, 150.82, 148.04, 137.15, 127.03 (q, $J = 275$ Hz), 125.40, 117.11, 103.62, 55.88, 44.45, 41.06, 34.45, 29.60 (q, $J = 29$ Hz), 29.38, 28.85, 25.95 (q, $J = 2.8$ Hz). $t_{\text{RLCMS}} = 6.3$ min. Purity >99%. MS $[M + H]^+$ m/z 441.

4,4,4-Trifluoro-1-[4-(3-phenyl-1,2,4-oxadiazol-5-yl)piperidin-1-yl]butan-1-one (8). White powder. Yield 43%. ^1H NMR (CDCl₃) δ 8.08 (dd, $J = 7.8$ Hz, $J = 1.8$ Hz, 2H), 7.46–7.53 (m, 3H), 4.48–4.53 (m, 1H), 3.90–3.95 (m, 1H), 3.27–3.35 (m, 2H), 3.00–3.09 (m, 1H), 2.51–2.63 (m, 4H), 2.18–2.23 (m, 2H), 1.91–2.02 (m, 2H). ^{13}C NMR (CDCl₃) δ 180.65, 168.34, 168.08, 131.29, 128.90, 127.43, 126.65, 127.08 (q, $J = 275$ Hz), 44.43, 41.02, 34.22, 29.61 (q, $J = 29$ Hz), 29.49, 28.90, 25.95 (q, $J = 2.9$ Hz). $t_{\text{RLCMS}} = 6.3$ min. Purity >99%. MS $[M + H]^+$ m/z 354.

4,4,4-Trifluoro-1-[4-(3-pyrazin-2-yl-1,2,4-oxadiazol-5-yl)piperidin-1-yl]butan-1-one (9). Colorless oil. Yield 37%. ^1H NMR (acetone) δ 9.26 (d, $J = 1.1$ Hz, 1H), 8.80–8.83 (m, 2H), 4.49–4.54 (m, 1H), 4.09–4.14 (m, 1H), 3.48–3.58 (m, 1H), 3.37–3.46 (m, 1H), 2.97–3.06 (m, 1H), 2.71–2.78 (m, 2H), 2.49–2.60 (m, 2H), 2.21–2.31 (m, 2H), 1.93–2.02 (m, 1H), 1.84–1.89 (m, 1H). ^{13}C NMR (acetone) δ 183.49, 168.56, 167.29, 147.68, 145.93, 144.91, 143.37, 128.61 (q, $J = 275$ Hz), 44.93, 41.46, 34.97, 30.25, 29.98 (q, $J = 29$ Hz), 29.71, 26.16 (q, $J = 2.8$ Hz). $t_{\text{RLCMS}} = 4.8$ min. Purity >99%. MS $[M + H]^+$ m/z 356.

4,4,4-Trifluoro-1-[4-(3-pyrimidin-2-yl-1,2,4-oxadiazol-5-yl)piperidin-1-yl]butan-1-one (10). White powder. Yield 55%. ^1H NMR (CD₂Cl₂) δ 8.95 (d, $J = 4.8$ Hz, 2H), 7.48 (t, $J = 4.8$ Hz, 1H), 4.51–4.56 (m, 1H), 3.91–3.96 (m, 1H), 3.25–3.40 (m, 2H), 2.93–3.02 (m, 1H), 2.50–2.66 (m, 4H), 2.22–2.29 (m, 2H), 1.96–2.02 (m, 2H). $t_{\text{RLCMS}} = 4.4$ min. Purity >99%. MS $[M + H]^+$ m/z 356.

4,4,4-Trifluoro-1-[4-(3-pyridin-2-yl-1,2,4-oxadiazol-5-yl)piperidin-1-yl]butan-1-one (11). White powder. Yield 35%. ^1H

NMR (CD₂Cl₂) δ 8.77 (ddd, $J = 4.8$ Hz, $J = 1.8$ Hz, $J = 0.9$ Hz, 1H), 8.12 (ddd, $J = 8.1$ Hz, $J = 1.2$ Hz, $J = 0.9$ Hz, 1H), 7.88 (td, $J = 7.8$ Hz, $J = 1.8$ Hz, 1H), 7.46 (ddd, $J = 7.5$ Hz, $J = 4.8$ Hz, $J = 1.2$ Hz, 1H), 4.49–4.53 (m, 1H), 3.91–3.95 (m, 1H), 3.26–3.39 (m, 2H), 2.94–3.04 (m, 1H), 2.45–2.66 (m, 4H), 2.19–2.28 (m, 2H), 1.83–2.04 (m, 2H). $t_{R,LCSMS} = 4.7$ min. Purity >99%. MS [M + H]⁺ m/z 355.

4,4,4-Trifluoro-1-[4-(3-pyridin-3-yl)-1,2,4-oxadiazol-5-yl]piperidin-1-yl]butan-1-one (12). White powder. Yield 40%. ¹H NMR (CDCl₃) δ 9.29 (d, $J = 1.5$ Hz, 1H), 8.74 (dd, $J = 4.8$ Hz, $J = 1.5$ Hz, 1H), 8.33 (dt, $J = 8.0$ Hz, $J = 1.8$ Hz, 1H), 7.42 (ddd, $J = 8.0$ Hz, $J = 4.8$ Hz, $J = 0.8$ Hz, 1H), 4.48–4.53 (m, 1H), 3.89–3.95 (m, 1H), 3.26–3.35 (m, 2H), 2.97–3.06 (m, 1H), 2.47–2.64 (m, 4H), 2.17–2.26 (m, 2H), 1.87–2.04 (m, 2H). $t_{R,LCSMS} = 4.7$ min. Purity >99%. MS [M + H]⁺ m/z 355.

4,4,4-Trifluoro-1-[4-(3-pyridin-4-yl)-1,2,4-oxadiazol-5-yl]piperidin-1-yl]butan-1-one (13). White powder. Yield 59%. ¹H NMR (CD₂Cl₂) δ 8.74 (dd, $J = 4.4$ Hz, $J = 1.7$ Hz, 2H), 7.90 (dd, $J = 4.4$ Hz, $J = 1.7$ Hz, 2H), 4.48–4.52 (m, 1H), 3.85–3.91 (m, 1H), 3.21–3.35 (m, 2H), 2.91–3.00 (m, 1H), 2.41–2.63 (m, 4H), 2.14–2.23 (m, 2H), 1.78–1.98 (m, 2H). $t_{R,LCSMS} = 4.7$ min. Purity >99%. MS [M + H]⁺ m/z 355.

4,4,4-Trifluoro-1-[4-[3-(2-fluorophenyl)-1,2,4-oxadiazol-5-yl]piperidin-1-yl]butan-1-one (14). White powder. Yield 78%. ¹H NMR (CDCl₃) δ 8.06 (td, $J = 7.5$ Hz, $J = 1.7$ Hz, 1H), 7.48–7.56 (m, 1H), 7.22–7.33 (m, 2H), 4.50–4.55 (m, 1H), 3.92–3.96 (m, 1H), 3.28–3.37 (m, 2H), 3.00–3.09 (m, 1H), 2.48–2.67 (m, 4H), 2.06–2.28 (m, 2H), 1.67–1.87 (m, 2H). ¹³C NMR (CDCl₃) δ 180.33, 167.99, 165.04 (d, $J = 5.1$ Hz), 160.57 (d, $J = 257$ Hz), 132.78 (d, $J = 8.6$ Hz), 130.67, 127.08 (q, $J = 275$ Hz), 124.42, 116.60 (d, $J = 21$ Hz), 114.91 (d, $J = 12$ Hz), 44.31, 40.91, 34.05, 29.50 (q, $J = 29$ Hz), 29.39, 28.80, 25.80. $t_{R,LCSMS} = 5.7$ min. Purity >99%. MS [M + H]⁺ m/z 372.

4,4,4-Trifluoro-1-[4-[3-(3-fluorophenyl)-1,2,4-oxadiazol-5-yl]piperidin-1-yl]butan-1-one (15). White powder. Yield 68%. ¹H NMR (CDCl₃) δ 7.87–7.90 (m, 1H), 7.77–7.81 (m, 1H), 7.44–7.52 (m, 1H), 7.19–7.26 (m, 1H), 4.48–4.56 (m, 1H), 3.91–3.98 (m, 1H), 3.26–3.37 (m, 2H), 3.00–3.09 (m, 1H), 2.49–2.67 (m, 4H), 2.18–2.28 (m, 2H), 1.86–2.06 (m, 2H). ¹³C NMR (CDCl₃) δ 180.98, 168.06, 167.43, 162.84 (d, $J = 246$ Hz), 130.60 (d, $J = 7.9$ Hz), 128.71 (d, $J = 8.3$ Hz), 127.06 (q, $J = 275$ Hz), 123.12, 118.22 (d, $J = 21$ Hz), 114.44 (d, $J = 23$ Hz), 44.36, 40.96, 34.18, 29.56 (q, $J = 29$ Hz), 29.42, 28.83, 25.89. $t_{R,LCSMS} = 6.5$ min. Purity >99%. MS [M + H]⁺ m/z 372.

4,4,4-Trifluoro-1-[4-[3-(4-fluorophenyl)-1,2,4-oxadiazol-5-yl]piperidin-1-yl]butan-1-one (16). White powder. Yield 84%. ¹H NMR (CDCl₃) δ 8.06–8.11 (m, 2H), 7.16–7.21 (m, 2H), 4.50–4.54 (m, 1H), 3.91–3.96 (m, 1H), 3.26–3.37 (m, 2H), 3.00–3.09 (m, 1H), 2.48–2.66 (m, 4H), 2.19–2.27 (m, 2H), 1.85–2.05 (m, 2H). ¹³C NMR (CDCl₃) δ 180.82, 167.97, 167.39, 164.50 (d, $J = 251$ Hz), 129.51 (d, $J = 8.3$ Hz), 127.09 (q, $J = 275$ Hz), 122.94, 115.96 (d, $J = 22$ Hz), 44.30, 40.91, 34.11, 29.50 (q, $J = 29$ Hz), 29.39, 28.79, 25.81. $t_{R,LCSMS} = 6.5$ min. Purity >99%. MS [M + H]⁺ m/z 372.

1-[4-[3-(2-Chlorophenyl)-1,2,4-oxadiazol-5-yl]piperidin-1-yl]-4,4,4-trifluorobutan-1-one (17). White powder. Yield 30%. ¹H NMR (CD₂Cl₂) δ 7.92–7.96 (m, 1H), 7.56–7.59 (m, 1H), 7.41–7.52 (m, 2H), 4.47–4.51 (m, 1H), 3.90–3.95 (m, 1H), 3.26–3.39 (m, 2H), 2.97–3.06 (m, 1H), 2.47–2.66 (m, 4H), 2.18–2.23 (m, 2H), 1.83–2.02 (m, 2H). $t_{R,LCSMS} = 6.4$ min. Purity >99%. MS [M + H]⁺ m/z 388.

1-[4-[3-(3-Chlorophenyl)-1,2,4-oxadiazol-5-yl]piperidin-1-yl]-4,4,4-trifluoro-butan-1-one (18). White powder. Yield 80%. ¹H NMR (CDCl₃) δ 8.09 (t, $J = 1.7$ Hz, 1H), 7.98 (dt, $J = 7.5$ Hz, $J = 1.4$ Hz, 1H), 7.51 (ddd, $J = 8.0$ Hz, $J = 1.5$ Hz, $J = 1.4$ Hz, 1H), 7.44 (dd, $J = 8.0$ Hz, $J = 7.5$ Hz, 1H), 4.48–4.55 (m, 1H), 3.90–3.98 (m, 1H), 3.26–3.37 (m, 2H), 3.00–3.09 (m, 1H), 2.49–2.67 (m, 4H), 2.18–2.28 (m, 2H), 1.86–2.06 (m, 2H). $t_{R,LCSMS} = 7.0$ min. Purity >99%. MS [M + H]⁺ m/z 388.

1-[4-[3-(4-Chlorophenyl)-1,2,4-oxadiazol-5-yl]piperidin-1-yl]-4,4,4-trifluorobutan-1-one (19). White powder. Yield 77%. ¹H NMR (CDCl₃) δ 8.02 (d, $J = 8.5$ Hz, 2H), 7.48 (d, $J = 8.5$ Hz, 2H), 4.49–4.56 (m, 1H), 3.90–3.97 (m, 1H), 3.25–3.37 (m, 2H), 3.00–3.09 (m, 1H), 2.49–2.67 (m, 4H), 2.18–2.27 (m, 2H), 1.85–2.05 (m, 2H). $t_{R,LCSMS} = 7.0$ min. Purity >99%. MS [M + H]⁺ m/z 388.

4,4,4-Trifluoro-1-[4-(3-*o*-tolyl)-1,2,4-oxadiazol-5-yl]piperidin-1-yl]butan-1-one (20). Colorless oil. Yield 64%. ¹H NMR (CDCl₃) δ 7.97–8.00 (m, 1H), 7.29–7.43 (m, 3H), 4.46–4.53 (m, 1H), 3.89–3.95 (m, 1H), 3.26–3.37 (m, 2H), 3.02–3.11 (m, 1H), 2.63 (s, 3H), 2.47–2.66 (m, 4H), 2.19–2.26 (m, 2H), 1.87–2.06 (m, 2H). ¹³C NMR (CDCl₃) δ 179.61, 168.82, 168.01, 138.15, 131.39, 130.61, 129.99, 127.10 (q, $J = 275$ Hz), 125.96, 44.33, 40.95, 34.02, 29.56 (q, $J = 29$ Hz), 29.45, 28.85, 25.86, 22.08. $t_{R,LCSMS} = 6.6$ min. Purity >99%. MS [M + H]⁺ m/z 368.

4,4,4-Trifluoro-1-[4-(3-*m*-tolyl)-1,2,4-oxadiazol-5-yl]piperidin-1-yl]butan-1-one (21). Colorless oil. Yield 78%. ¹H NMR (CDCl₃) δ 7.86–7.89 (m, 2H), 7.31–7.40 (m, 2H), 4.48–4.53 (m, 1H), 3.90–3.95 (m, 1H), 3.25–3.36 (m, 2H), 3.00–3.09 (m, 1H), 2.49–2.66 (m, 4H), 2.44 (s, 3H), 2.17–2.26 (m, 2H), 1.86–2.05 (m, 2H). ¹³C NMR (CDCl₃) δ 180.62, 168.31, 168.02, 138.66, 132.00, 128.75, 127.88, 127.09 (q, $J = 275$ Hz), 126.51, 124.46, 44.34, 40.95, 34.14, 29.53 (q, $J = 29$ Hz), 29.41, 28.81, 25.82, 21.23. $t_{R,LCSMS} = 6.8$ min. Purity >99%. MS [M + H]⁺ m/z 368.

4,4,4-Trifluoro-1-[4-(3-*p*-tolyl)-1,2,4-oxadiazol-5-yl]piperidin-1-yl]butan-1-one (22). White powder. Yield 75%. ¹H NMR (CDCl₃) δ 7.96 (d, $J = 8.1$ Hz, 2H), 7.29 (d, $J = 8.1$ Hz, 2H), 4.47–4.52 (m, 1H), 3.90–3.94 (m, 1H), 3.24–3.35 (m, 2H), 3.00–3.09 (m, 1H), 2.49–2.65 (m, 4H), 2.43 (s, 3H), 2.17–2.25 (m, 2H), 1.85–2.04 (m, 2H). ¹³C NMR (CDCl₃) δ 180.51, 168.23, 167.97, 141.58, 129.57, 127.30, 127.10 (q, $J = 275$ Hz), 123.85, 44.33, 40.94, 34.13, 29.54 (q, $J = 29$ Hz), 29.42, 28.82, 25.84, 21.44. $t_{R,LCSMS} = 6.8$ min. Purity >99%. MS [M + H]⁺ m/z 368.

4,4,4-Trifluoro-1-[4-[3-(2-methoxyphenyl)-1,2,4-oxadiazol-5-yl]piperidin-1-yl]butan-1-one (23). Colorless oil. Yield 53%. ¹H NMR (CD₂Cl₂) δ 7.92 (dd, $J = 7.8$ Hz, $J = 1.8$ Hz, 1H), 7.44–7.50 (m, 1H), 7.02–7.08 (m, 2H), 4.41–4.48 (m, 1H), 3.91 (s, 3H), 3.85–3.91 (m, 1H), 3.21–3.31 (m, 2H), 2.91–3.00 (m, 1H), 2.43–2.61 (m, 4H), 2.12–2.21 (m, 2H), 1.77–1.97 (m, 2H). $t_{R,LCSMS} = 5.7$ min. Purity >99%. MS [M + H]⁺ m/z 384.

4,4,4-Trifluoro-1-[4-[3-(3-methoxyphenyl)-1,2,4-oxadiazol-5-yl]piperidin-1-yl]butan-1-one (24). Colorless oil. Yield 69%. ¹H NMR (CDCl₃) δ 7.68 (dt, $J = 7.6$ Hz, $J = 1.1$ Hz, 1H), 7.61 (dd, $J = 2.5$ Hz, $J = 1.5$ Hz, 1H), 7.41 (t, $J = 8.0$ Hz, 1H), 7.07 (ddd, $J = 8.3$ Hz, $J = 2.5$ Hz, $J = 1.0$ Hz, 1H), 4.48–4.55 (m, 1H), 3.90–3.98 (m, 1H), 3.90 (s, 3H), 3.26–3.36 (m, 2H), 3.00–3.09 (m, 1H), 2.48–2.66 (m, 4H), 2.18–2.27 (m, 2H), 1.87–2.06 (m, 2H). $t_{R,LCSMS} = 6.3$ min. Purity >99%. MS [M + H]⁺ m/z 384.

4,4,4-Trifluoro-1-[4-[3-(4-methoxyphenyl)-1,2,4-oxadiazol-5-yl]piperidin-1-yl]butan-1-one (25). White powder. Yield 82%. ¹H NMR (CDCl₃) δ 8.02 (d, $J = 9.0$ Hz, 2H), 7.00 (d, $J = 9.0$ Hz, 2H), 4.47–4.54 (m, 1H), 3.89–3.96 (m, 1H), 3.89 (s, 3H), 3.24–3.36 (m, 2H), 3.00–3.09 (m, 1H), 2.48–2.67 (m, 4H), 2.17–2.26 (m, 2H), 1.86–2.05 (m, 2H). $t_{R,LCSMS} = 6.3$ min. Purity >99%. MS [M + H]⁺ m/z 384.

4,4,4-Trifluoro-1-[4-[3-(2-trifluoromethylphenyl)-1,2,4-oxadiazol-5-yl]piperidin-1-yl]butan-1-one (26). Colorless oil. Yield 58%. ¹H NMR (CDCl₃) δ 7.78–7.87 (m, 2H), 7.62–7.70 (m, 2H), 4.40–4.44 (m, 1H), 3.88–3.92 (m, 1H), 3.29–3.39 (m, 2H), 3.07–3.16 (m, 1H), 2.47–2.65 (m, 4H), 2.18–2.27 (m, 2H), 1.87–2.06 (m, 2H). $t_{R,LCSMS} = 6.6$ min. Purity 99%. MS [M + H]⁺ m/z 422.

4,4,4-Trifluoro-1-[4-[3-(3-trifluoromethylphenyl)-1,2,4-oxadiazol-5-yl]piperidin-1-yl]butan-1-one (27). White powder. Yield 51%. ¹H NMR (CDCl₃) δ 8.34 (s, 1H), 8.26 (d, $J = 7.8$ Hz, 1H), 7.76 (d, $J = 7.8$ Hz, 1H), 7.62 (t, $J = 7.8$ Hz, 1H), 4.48–4.54 (m, 1H), 3.89–3.95 (m, 1H), 3.26–3.35 (m, 2H), 2.98–3.07 (m, 1H), 2.44–2.65 (m, 4H), 2.17–2.26 (m, 2H), 1.85–2.05 (m, 2H). $t_{R,LCSMS} = 6.5$ min. Purity >99%. MS [M + H]⁺ m/z 422.

4,4,4-Trifluoro-1-[4-[3-(4-trifluoromethylphenyl)-1,2,4-oxadiazol-5-yl]piperidin-1-yl]butan-1-one (28). White powder. Yield 30%. ¹H NMR (MeOD) δ 8.26 (d, $J = 8.1$ Hz, 2H), 7.84 (d, $J = 8.1$ Hz, 2H), 4.45–4.50 (m, 1H), 4.01–4.06 (m, 1H), 3.36–3.49 (m, 2H), 3.00–3.10 (m, 1H), 2.71–2.76 (m, 2H), 2.44–2.61 (m, 2H), 2.19–2.27 (m, 2H), 1.78–2.04 (m, 2H). $t_{R,LCSMS} = 7.2$ min. Purity >99%. MS [M + H]⁺ m/z 422.

4,4,4-Trifluoro-1-[4-[3-(4-hydroxyphenyl)-1,2,4-oxadiazol-5-yl]piperidin-1-yl]butan-1-one (29). Beige powder. Yield 42%. ¹H

NMR (CDCl₃) δ 7.95 (d, J = 8.7 Hz, 2H), 6.94 (d, J = 8.7 Hz, 2H), 6.64 (brs, OH), 4.46–4.52 (m, 1H), 3.90–3.95 (m, 1H), 3.23–3.37 (m, 2H), 3.01–3.11 (m, 1H), 2.45–2.67 (m, 4H), 2.16–2.25 (m, 2H), 1.85–2.04 (m, 2H). $t_{R,LCSMS}$ = 5.0 min. Purity 96%. MS [M + H]⁺ m/z 370.

1-[4-[3-(4-Dimethylaminophenyl)-1,2,4-oxadiazol-5-yl]piperidin-1-yl]-4,4,4-trifluorobutan-1-one (30). Beige powder. Yield 31%. ¹H NMR (CDCl₃) δ 7.93 (d, J = 9.1 Hz, 2H), 6.76 (d, J = 9.1 Hz, 2H), 4.48–4.52 (m, 1H), 3.90–3.95 (m, 1H), 3.22–3.35 (m, 2H), 3.00–3.09 (m, 1H), 3.05 (s, 6H), 2.48–2.66 (m, 4H), 2.16–2.25 (m, 2H), 1.86–2.05 (m, 2H). $t_{R,LCSMS}$ = 6.0 min. Purity 99%. MS [M + H]⁺ m/z 397.

1-[4-[3-(4-*tert*-Butylphenyl)-1,2,4-oxadiazol-5-yl]piperidin-1-yl]-4,4,4-trifluorobutan-1-one (31). White powder. Yield 40%. ¹H NMR (MeOD) δ 7.98 (d, J = 12.9 Hz, 2H), 7.56 (d, J = 12.9 Hz, 2H), 4.44–4.49 (m, 1H), 4.00–4.05 (m, 1H), 3.35–3.45 (m, 2H), 2.98–3.08 (m, 1H), 2.70–2.76 (m, 2H), 2.44–2.60 (m, 2H), 2.16–2.25 (m, 2H), 1.77–2.00 (m, 2H), 1.36 (s, 9H). $t_{R,LCSMS}$ = 7.9 min. Purity >99%. MS [M + H]⁺ m/z 410.

1-[4-(3-Cyclopentyl-1,2,4-oxadiazol-5-yl)piperidin-1-yl]-4,4,4-trifluorobutan-1-one (32). Colorless oil. Yield 45%. ¹H NMR (CDCl₃) δ 4.43–4.48 (m, 1H), 3.84–3.89 (m, 1H), 3.12–3.29 (m, 3H), 2.91–3.00 (m, 1H), 2.42–2.61 (m, 4H), 1.97–2.16 (m, 4H), 1.63–1.92 (m, 8H). ¹³C NMR (CDCl₃) δ 180.15, 173.91, 167.96, 127.02 (q, J = 275 Hz), 44.37, 40.96, 36.50, 34.12, 31.26, 29.49 (q, J = 29 Hz), 29.39, 28.82, 25.78, 25.44. $t_{R,LCSMS}$ = 5.7 min. Purity >99%. MS [M + H]⁺ m/z 346.

1-[4-(3-Cyclohexyl-1,2,4-oxadiazol-5-yl)piperidin-1-yl]-4,4,4-trifluorobutan-1-one (33). Colorless oil. Yield 45%. ¹H NMR (CDCl₃) δ 4.42–4.49 (m, 1H), 3.84–3.88 (m, 1H), 3.12–3.29 (m, 2H), 2.91–3.00 (m, 1H), 2.71–2.81 (m, 1H), 2.41–2.61 (m, 4H), 2.08–2.17 (m, 2H), 1.93–1.97 (m, 2H), 1.70–1.89 (m, 5H), 1.25–1.61 (m, 5H). ¹³C NMR (CDCl₃) δ 179.95, 174.00, 168.00, 127.02 (q, J = 275 Hz), 44.40, 40.99, 35.82, 34.13, 30.51, 29.52 (q, J = 29 Hz), 29.41, 28.84, 25.81, 25.66, 25.60. $t_{R,LCSMS}$ = 6.1 min. Purity >99%. MS [M + H]⁺ m/z 360.

4,4,4-Trifluoro-1-[4-(4-thiophen-2-ylthiazol-2-yl)piperidin-1-yl]butan-1-one (34). 2-Bromo-1-thiophen-2-ylethanone (2.00 g, 9.75 mmol) and 4-thiocarbamoylpiperidine-1-carboxylic acid *tert*-butyl ester (2.38 g, 9.75 mmol) were mixed in 35 mL of THF. The mixture was heated at 70 °C overnight and then cooled to room temperature. The solution was filtered and then evaporated under reduced pressure to afford 2.75 g of 4-(4-thiophen-2-ylthiazol-2-yl)piperidine-1-carboxylic acid *tert*-butyl ester. This product was used in the next step without further purification. Boc intermediate (2.60 g, 7.42 mmol) was dissolved in dioxane (25 mL), and 4 N HCl solution in dioxane (8 equiv) was added. The reaction mixture was stirred overnight at room temperature. The product was recovered by filtration and then washed with petroleum ether to give 2.10 g of 4-(4-thiophen-2-ylthiazol-2-yl)piperidine hydrochloride (yield, 99%). 4,4,4-Trifluorobutyric acid (2 equiv), EDCI (2 equiv), and TEA (4 equiv) were mixed in DCM (8 mL) for 10 min. 4-(4-Thiophen-2-ylthiazol-2-yl)piperidine hydrochloride (150 mg, 0.5 mmol, 1 equiv) was added, and the reaction mixture was stirred overnight at room temperature and then evaporated under reduced pressure and purified by preparative HPLC to give **34** as a white powder. Yield 23%. ¹H NMR (CD₂Cl₂) δ 7.47 (dd, J = 3.6 Hz, J = 1.1 Hz, 1H), 7.32 (dd, J = 5.0 Hz, J = 1.1 Hz, 1H), 7.32 (s, 1H), 7.09 (dd, J = 5.0 Hz, J = 3.6 Hz, 1H), 4.63–4.67 (m, 1H), 3.94–3.98 (m, 1H), 3.20–3.32 (m, 2H), 2.85–2.90 (m, 1H), 2.45–2.66 (m, 4H), 2.17–2.27 (m, 2H), 1.70–1.90 (m, 2H). ¹³C NMR (CD₂Cl₂) δ 174.01, 167.72, 149.34, 138.45, 127.70, 127.43 (q, J = 275 Hz), 125.13, 123.87, 110.51, 45.00, 41.55, 40.41, 32.60, 32.03, 29.50 (q, J = 29 Hz), 25.81. $t_{R,LCSMS}$ = 6.4 min. Purity 99%. MS [M + H]⁺ m/z 375.

4,4,4-Trifluoro-1-[4-(5-thiophen-2-yl-1,2,4-oxadiazol-3-yl)piperidin-1-yl]butan-1-one (35). 4-Cyanopiperidine-1-carboxylic acid *tert*-butyl ester (1.50 g, 7.13 mmol), hydroxylamine hydrochloride (0.74 g, 10.70 mmol, 1.5 equiv), and DIEA (1.97 mL, 1.6 equiv) were mixed in 20 mL of EtOH. The mixture was heated for 5 h at reflux and then evaporated under reduced pressure. The residue was dissolved in

AcOEt, washed twice with water and once with brine. The organic layer was dried over MgSO₄ and then evaporated under reduced pressure to give 1.07 g of 4-(*N*-hydroxycarbamidoyl)piperidine-1-carboxylic acid *tert*-butyl ester. This product was used in the next step without further purification. Thiophene-2-carboxylic acid (527 mg, 1 equiv), HBTU (1 equiv), and DIEA (2.5 equiv) were dissolved in DMF (15 mL). The solution was stirred for 5 min, and then the amidoxime previously synthesized (1.00 g, 1 equiv) was added. The reaction mixture was stirred overnight at room temperature and then evaporated under reduced pressure. The residue was dissolved in AcOEt and washed once with brine, then dried over MgSO₄ and evaporated under reduced pressure. The residue was dissolved in dioxane (15 mL), and then the reaction mixture was heated 5 h at 110 °C. The solvent was removed under vacuum, and the residue was dissolved in AcOEt. The organic layer was washed twice with 1 N HCl, twice with saturated aqueous NaHCO₃ and twice with brine, then dried over MgSO₄, evaporated under reduced pressure, and purified by preparative HPLC to give 47 mg of 4-(5-thiophen-2-yl-1,2,4-oxadiazol-3-yl)piperidine-1-carboxylic acid *tert*-butyl ester. Boc intermediate (40 mg, 0.12 mmol) was dissolved in dioxane (1 mL), and 4 N HCl solution in dioxane (10 equiv) was added. The reaction mixture was stirred overnight at room temperature. The product was recovered by filtration and then washed with petroleum ether to give 30 mg of 4-(5-thiophen-2-yl-1,2,4-oxadiazol-3-yl)piperidine hydrochloride (yield, 92%). 4,4,4-Trifluorobutyric acid (2 equiv), EDCI (2 equiv), and TEA (4 equiv) were mixed in DCM (3 mL) for 5 min. 4-(5-Thiophen-2-yl-1,2,4-oxadiazol-3-yl)piperidine hydrochloride (25 mg, 0.09 mmol, 1 equiv) was added, and the reaction mixture was stirred overnight at room temperature and then evaporated under reduced pressure and purified by preparative HPLC to give **35** as a colorless oil. Yield 54%. ¹H NMR (CD₂Cl₂) δ 7.91 (d, J = 3.7 Hz, 1H), 7.71 (d, J = 5.0 Hz, 1H), 7.25 (dd, J = 5.0 Hz, J = 3.7 Hz, 1H), 4.53–4.58 (m, 1H), 3.90–3.95 (m, 1H), 3.09–3.31 (m, 2H), 2.87–2.96 (m, 1H), 2.46–2.67 (m, 4H), 2.10–2.17 (m, 2H), 1.74–1.94 (m, 2H). ¹³C NMR (CD₂Cl₂) δ 172.97, 171.16, 167.70, 131.97, 131.72, 128.59, 127.39 (q, J = 276 Hz), 125.82, 44.73, 41.25, 33.92, 29.80, 29.48 (q, J = 29 Hz), 29.28, 25.79. $t_{R,LCSMS}$ = 5.8 min. Purity 96%. MS [M + H]⁺ m/z 360.

4,4,4-Trifluoro-1-[4-(5-thiophen-2-yl-2H-pyrazol-3-yl)piperidin-1-yl]butan-1-one (36). 4,4,4-Trifluorobutyric acid (1.5 equiv), EDCI (1.5 equiv), and DIEA (4.5 equiv) were mixed in DMF (5 mL) for 5 min. 4-[5-(2-Thienyl)-1H-pyrazol-3-yl]piperidine (117 mg, 0.5 mmol, 1 equiv) was added, and the reaction mixture was stirred overnight at room temperature and then evaporated under reduced pressure. The residue was dissolved in AcOEt. The organic layer was washed twice with 1 N HCl, twice with saturated aqueous NaHCO₃, and twice with brine, then dried over MgSO₄, evaporated under reduced pressure, and purified by preparative HPLC to give **36** as a white powder. Yield 51%. ¹H NMR (CD₂Cl₂) δ 7.26 (d, J = 3.7 Hz, 1H), 7.21 (d, J = 5.0 Hz, 1H), 7.03 (dd, J = 5.0 Hz, J = 3.7 Hz, 1H), 6.24 (s, 1H), 4.48–4.52 (m, 1H), 3.64–3.68 (m, 1H), 2.74–2.94 (m, 2H), 2.43–2.54 (m, 5H), 1.90–1.94 (m, 2H), 1.43–1.56 (m, 2H). ¹³C NMR (CD₂Cl₂) δ 168.27, 150.32, 145.93, 136.71, 128.20, 127.94 (q, J = 275 Hz), 125.03, 124.29, 99.68, 45.58, 42.20, 34.28, 32.59, 31.62, 30.03 (q, J = 29 Hz), 26.34. $t_{R,LCSMS}$ = 5.5 min. Purity >99%. MS [M + H]⁺ m/z 358.

4,4,4-Trifluoro-1-[4-(4-phenylthiazol-2-yl)piperidin-1-yl]butan-1-one (37). 2-Bromo-1-phenylethanone (1.00 g, 5.0 mmol) and 4-thiocarbamoylpiperidine-1-carboxylic acid *tert*-butyl ester (1.23 g, 5.0 mmol) were mixed in 50 mL of THF. The mixture was heated at 70 °C overnight and then cooled to room temperature. The solution was filtered and then evaporated under reduced pressure to afford 1.65 g of 4-(4-phenylthiazol-2-yl)piperidine-1-carboxylic acid *tert*-butyl ester. This product was used in the next step without further purification. Boc intermediate (1.5 g, 4.35 mmol) was dissolved in dioxane (10 mL), and 4 N HCl solution in dioxane (8 equiv) was added. The reaction mixture was stirred overnight at room temperature. The product was recovered by filtration and then washed with petroleum ether to give 800 mg of 4-(4-phenylthiazol-2-yl)piperidine hydrochloride (yield, 65%). 4,4,4-Trifluorobutyric acid (2 equiv), EDCI (2 equiv), and TEA (4 equiv) were mixed in DCM (8 mL) for 10 min. 4-(4-Phenylthiazol-2-yl)piperidine

hydrochloride (150 mg, 0.53 mmol, 1 equiv) was added, and the reaction mixture was stirred overnight at room temperature and then evaporated under reduced pressure and purified by preparative HPLC to give **37** as a white powder. Yield 68%. $^1\text{H NMR}$ (CD_2Cl_2) δ 7.90–7.94 (m, 2H), 7.41–7.47 (m, 3H), 7.33–7.38 (m, 1H), 4.62–4.66 (m, 1H), 3.94–3.98 (m, 1H), 3.21–3.40 (m, 2H), 2.83–2.93 (m, 1H), 2.46–2.67 (m, 4H), 2.21–2.29 (m, 2H), 1.74–1.93 (m, 2H). $^{13}\text{C NMR}$ (CD_2Cl_2) δ 173.73, 167.73, 154.84, 134.59, 128.68, 127.99, 127.40 (q, $J = 275$ Hz), 126.21, 111.82, 45.01, 41.56, 40.47, 32.61, 32.04, 29.51 (q, $J = 29$ Hz), 25.80. $t_{\text{R,LCMS}} = 6.7$ min. Purity >99%. MS $[\text{M} + \text{H}]^+ m/z$ 369.

4,4,4-Trifluoro-1-[4-(5-phenyl-1,3,4-oxadiazol-2-yl)-piperidin-1-yl]butan-1-one (38). 4,4,4-Trifluorobutyric acid (1.5 equiv), EDCI (1.5 equiv), and DIEA (4.5 equiv) were mixed in DMF (5 mL) for 5 min. 4-(5-Phenyl-1,3,4-oxadiazol-2-yl)piperidine (115 mg, 0.5 mmol, 1 equiv) was added, and the reaction mixture was stirred overnight at room temperature and then evaporated under reduced pressure. The residue was dissolved in AcOEt. The organic layer was washed twice with 1 N HCl, twice with saturated aqueous NaHCO_3 , and twice with brine, then dried over MgSO_4 , evaporated under reduced pressure, and purified by preparative HPLC to give **38** as a white powder. Yield 48%. $^1\text{H NMR}$ (CD_2Cl_2) δ 7.99–8.01 (m, 2H), 7.50–7.52 (m, 3H), 4.43–4.48 (m, 1H), 3.86–3.91 (m, 1H), 3.20–3.29 (m, 2H), 2.91–3.00 (m, 1H), 2.45–2.62 (m, 4H), 2.12–2.21 (m, 2H), 1.76–1.96 (m, 2H). $^{13}\text{C NMR}$ (CD_2Cl_2) δ 168.58, 168.28, 165.20, 132.12, 129.55, 127.88 (q, $J = 275$ Hz), 127.16, 124.55, 44.92, 41.44, 33.80, 29.97 (q, $J = 29$ Hz), 29.90, 29.38, 26.29 (q, $J = 2.9$ Hz). $t_{\text{R,LCMS}} = 5.2$ min. Purity >99%. MS $[\text{M} + \text{H}]^+ m/z$ 354.

4,4,4-Trifluoro-1-[4-(3-phenylisoxazol-5-yl)piperidin-1-yl]butan-1-one (39). Benzenesulfonyl chloride (2 mL, 15.6 mmol, 1 equiv) was dissolved in 30 mL of acetone, and the solution was cooled to 0 °C. Sodium azide (1.52 g, 1.5 equiv) dissolved in 5 mL of water was added dropwise to the solution. The reaction mixture was stirred for 3 h at room temperature and then evaporated under reduced pressure. The residue was dissolved in 20 mL of water, and the aqueous phase was extracted three times with diethyl ether. The organic phases were joined, dried over MgSO_4 , and then evaporated under reduced pressure to give 2.73 g of benzenesulfonyl azide (yield, 94%). Sodium hydride (60% in mineral oil) (330 mg, 8.2 mmol, 1.5 equiv) was added to 19 mL of THF, and the mixture was cooled to 0 °C and stirred 5 min under nitrogen. Methyl diethylphosphonoacetate (1.5 mL, 1.5 equiv) dissolved in 2.5 mL of THF was added dropwise to the solution. The reaction mixture was stirred for 10 min at 0 °C, and then benzenesulfonylazide (1.0 g, 5.4 mmol) dissolved in 2.5 mL of THF was added dropwise to the solution and the reaction mixture was stirred 1 h at 0 °C. A yellow precipitate was observed. An amount of 2 mL of aqueous 5% NaHCO_3 was added to dissolve the precipitate, and then THF was removed under reduced pressure. The residue was dissolved in AcOEt. The organic layer was washed once with aqueous 5% NaHCO_3 , three times with water, then dried over MgSO_4 and evaporated under reduced pressure. A mixture of petroleum ether/AcOEt (95/5) was added to the residue. The precipitate of benzenesulfonamide was removed by filtration, and then the solution was evaporated under reduced pressure to give 580 mg of diazo-(diethoxyphosphoryl)acetic acid methyl ester (yield, 45%). 4-Formylpiperidine-1-carboxylic acid *tert*-butyl ester (524 mg, 2.45 mmol, 1 equiv) and K_2CO_3 (2 equiv) were mixed in 15 mL of MeOH. Diazo-(diethoxyphosphoryl)acetic acid methyl ester (580 mg, 2.45 mmol, 1 equiv) dissolved in 10 mL of MeOH was added to the solution, and the reaction mixture was stirred overnight at room temperature and then evaporated under reduced pressure. The residue was dissolved in diethyl ether. The organic layer was washed twice with aqueous 5% NaHCO_3 , then dried over MgSO_4 and evaporated under reduced pressure to give 685 mg of 4-ethynylpiperidine-1-carboxylic acid *tert*-butyl ester.²⁵ Benzaldehyde oxime (261 μL , 2.39 mmol) and 4-ethynylpiperidine-1-carboxylic acid *tert*-butyl ester (500 mg, 2.39 mmol) were mixed in 5 mL of DCM. The mixture was cooled to 0 °C, and then a sodium hypochlorite solution (14% chlorine, 8 mL) was added dropwise to the solution. The reaction mixture was stirred overnight at room temperature, and then an amount of 20 mL of DCM was added. The organic layer was washed once with water, once

with 1 N HCl, once with saturated aqueous NaHCO_3 , once with brine, then dried over MgSO_4 and evaporated under reduced pressure to afford 700 mg of 4-(3-phenylisoxazol-5-yl)piperidine-1-carboxylic acid *tert*-butyl ester. This product was used in the next step without further purification. Boc intermediate (700 mg, 2.13 mmol) was dissolved in dioxane (9 mL), and 4 N HCl solution in dioxane (8 equiv) was added. The reaction mixture was stirred overnight at room temperature. The product was recovered by filtration and then washed with petroleum ether to give 220 mg of 4-(3-phenylisoxazol-5-yl)piperidine hydrochloride (yield 39% over two steps). 4,4,4-Trifluorobutyric acid (1.5 equiv), EDCI (1.5 equiv), HOBt (1 equiv), and DIEA (4 equiv) were mixed in DCM (8 mL) for 10 min. 4-(3-Phenylisoxazol-5-yl)piperidine hydrochloride (100 mg, 0.38 mmol, 1 equiv) was added with 1 mL of DMF, and the reaction mixture was stirred overnight at room temperature and then evaporated under reduced pressure and purified by preparative HPLC to give **39** as a white powder. Yield 20%. $^1\text{H NMR}$ (CDCl_3) δ 7.77–7.81 (m, 2H), 7.45–7.49 (m, 3H), 6.31 (s, 1H), 4.63–4.67 (m, 1H), 3.91–3.96 (m, 1H), 3.20–3.30 (m, 1H), 3.07–3.16 (m, 1H), 2.82–2.91 (m, 1H), 2.45–2.65 (m, 4H), 2.13–2.23 (m, 2H), 1.66–1.81 (m, 2H). $^{13}\text{C NMR}$ (CDCl_3) δ 175.42, 168.09, 162.37, 130.03, 129.03, 128.93, 126.96 (q, $J = 275$ Hz), 126.75, 97.89, 44.91, 41.51, 34.56, 30.59, 29.71, 29.64 (q, $J = 29$ Hz), 25.93. $t_{\text{R,LCMS}} = 6.3$ min. Purity >99%. MS $[\text{M} + \text{H}]^+ m/z$ 353.

3-Phenyl-1-[1-(4,4,4-trifluorobutanoyl)piperidin-4-yl]-4,5-dihydro-1H-pyrazol-5-one (40). Ethyl benzoylacetate (174 μL , 1 mmol) and 4-hydrazinopiperidine dihydrochloride (188 mg, 1 mmol) were mixed in a sealed microwave glass tube with 2 mL of EtOH. The reaction mixture was heated under microwave irradiation (50 W) for 45 min. The reaction was performed twice using a Discover microwave from CEM. The two reaction mixtures were put together, and then the solvent was removed under reduced pressure and the residue was purified by preparative HPLC to give 150 mg of 3-phenyl-1-(piperidin-4-yl)-4,5-dihydro-1H-pyrazol-5-one (yield, 31%). 4,4,4-Trifluorobutyric acid (1 equiv), EDCI (1 equiv), and DIEA (3 equiv) were mixed in DMF (3 mL) and then added dropwise to a solution of 3-phenyl-1-(piperidin-4-yl)-4,5-dihydro-1H-pyrazol-5-one (117 mg, 0.5 mmol, 1 equiv) in DMF (2 mL). The reaction mixture was stirred overnight at room temperature and then evaporated under reduced pressure and purified by preparative HPLC to give **40** as a white powder. Yield 62%. $^1\text{H NMR}$ (CD_2Cl_2) δ 7.69–7.72 (m, 2H), 7.44–7.47 (m, 3H), 4.68–4.75 (m, 1H), 4.33–4.43 (m, 1H), 3.94–4.00 (m, 1H), 3.67 (s, 2H), 3.18–3.27 (m, 1H), 2.73–2.83 (m, 1H), 2.49–2.69 (m, 4H), 1.86–2.06 (m, 4H). $^{13}\text{C NMR}$ (CD_2Cl_2) δ 171.02, 167.70, 154.02, 131.36, 130.14, 128.76, 127.38 (q, $J = 275$ Hz), 125.55, 50.45, 44.42, 41.07, 38.64, 30.48, 29.80, 29.50 (q, $J = 29$ Hz), 25.77 (q, $J = 2.9$ Hz). $t_{\text{R,LCMS}} = 5.1$ min. Purity 97%. MS $[\text{M} + \text{H}]^+ m/z$ 368.

4,4,4-Trifluoro-1-[(3R)-3-[3-(1,3-thiazol-2-yl)-1,2,4-oxadiazol-5-yl]pyrrolidin-1-yl]butan-1-one (41). (R)-*N*-Boc-pyrrolidine-3-carboxylic acid (700 mg, 3.25 mmol, 1.1 equiv), HBTU (1.23 g, 1.1 equiv), and DIEA (1.53 mL, 3 equiv) were dissolved in DMF (15 mL). The solution was stirred for 5 min, and then 1,3-thiazole-2-amidoxime (**5a**) (422 mg, 2.95 mmol, 1 equiv) was added. The reaction mixture was stirred overnight at room temperature and then evaporated under reduced pressure. The residue was dissolved in AcOEt, washed twice with saturated aqueous NaHCO_3 , once with brine, then dried over MgSO_4 and evaporated under reduced pressure. The residue was dissolved in 15 mL of DMF and then heated at 110 °C for 7 h. The solvent was removed under vacuum and the residue was dissolved in AcOEt. The organic layer was washed once with 1 N HCl, once with saturated aqueous NaHCO_3 , and once with brine, then dried over MgSO_4 and evaporated under reduced pressure. The obtained product was used in the next step without further purification. Boc intermediate was dissolved in dioxane (10 mL), and 4 N HCl solution in dioxane (6 mL) was added. The reaction mixture was stirred overnight at room temperature, and then the product was recovered by filtration and washed with petroleum ether to give 5-[(3R)-pyrrolidin-3-yl]-3-(1,3-thiazol-2-yl)-1,2,4-oxadiazole (yield, 66% over two steps). 4,4,4-Trifluorobutyric acid (1.3 equiv), EDCI (1.3 equiv), HOBt (0.4 equiv), and DIEA (4 equiv) were mixed in DMF (2 mL) for 5 min. 5-[(3R)-Pyrrolidin-3-yl]-3-(1,3-thiazol-2-yl)-1,2,4-oxadiazole (0.62 mmol,

1 equiv) was added with 3 mL of DMF. The reaction mixture was stirred overnight at room temperature and then evaporated under reduced pressure and purified by preparative HPLC. Beige powder. Yield 33%. $^1\text{H NMR}$ (CDCl_3) δ 8.02–8.00 (m, 1H), 7.57–7.60 (m, 1H), 3.89–4.03 (m, 2H), 3.69–3.87 (m, 2H), 3.53–3.65 (m, 1H), 2.38–2.55 (m, 6H). $^{13}\text{C NMR}$ (CDCl_3) cis/trans isomer mixture (60 isomer A/40 isomer B); isomer A δ 180.31, 168.50, 163.98, 153.53, 144.99, 126.94 (q, $J = 276$ Hz), 122.87, 49.24, 45.52, 35.03, 29.05 (q, $J = 29$ Hz), 28.86, 27.07 (q, $J = 3$ Hz); isomer B δ 179.84, 168.31, 163.98, 153.38, 144.94, 126.92 (q, $J = 276$ Hz), 122.81, 49.43, 45.25, 36.82, 30.28, 29.05 (q, $J = 29$ Hz), 27.24 (q, $J = 3$ Hz). $t_{\text{R,LCMS}} = 4.6$ min. Purity >99%. MS $[\text{M} + \text{H}]^+ m/z$ 347.

5,5,5-Trifluoro-1-[4-(3-thiazol-2-yl)-1,2,4-oxadiazol-5-yl]piperidin-1-yl]pentan-1-one (42). 5,5,5-Trifluoropentanoic acid (1.3 equiv), EDCI (1.3 equiv), HOBt (0.3 equiv), and DIEA (4 equiv) were mixed in DMF (40 mL) for 5 min. 4-(3-Thiazol-2-yl-[1,2,4]oxadiazol-5-yl)piperidine hydrochloride **5c** (8.18 g, 30 mmol, 1 equiv) was added with 20 mL of DMF, and the reaction mixture was stirred overnight at room temperature and then evaporated under reduced pressure. The residue was dissolved in AcOEt and then washed twice with saturated aqueous NaHCO_3 , twice with 1 N HCl, and once with brine, then dried over MgSO_4 and evaporated under reduced pressure. The residue was purified by chromatography on silica gel (DCM/MeOH, 100:0 to 98.5:1.5) and then recrystallized in a mixture of isopropanol and diisopropyl ether. White crystals. Yield 62%. $^1\text{H NMR}$ (CD_2Cl_2) δ 8.06 (d, $J = 3.0$ Hz, 1H), 7.65 (d, $J = 3.0$ Hz, 1H), 4.51–4.55 (m, 1H), 3.90–3.95 (m, 1H), 3.22–3.39 (m, 2H), 2.91–2.98 (m, 1H), 2.44 (t, $J = 7.2$ Hz, 2H), 2.15–2.27 (m, 4H), 1.83–2.01 (m, 4H). $^{13}\text{C NMR}$ (CDCl_3) δ 182.06, 169.56, 163.97, 154.00, 144.95, 127.37 (q, $J = 275$ Hz), 122.66, 44.33, 40.60, 34.43, 32.97 (q, $J = 29$ Hz), 31.34, 29.44, 28.90, 17.52. Mp 75.6–76.3 °C. $t_{\text{R,LCMS}} = 6.1$ min. Purity >99%. MS $[\text{M} + \text{H}]^+ m/z$ 375. HRMS calcd for $\text{C}_{15}\text{H}_{17}\text{F}_3\text{N}_4\text{O}_2\text{S}$ $[\text{M} + \text{H}]^+$, 375.1103; found, 375.1099.

■ ASSOCIATED CONTENT

Supporting Information

In vivo mouse AUC for compounds **2**, **5**, and **42**. This material is available free of charge via the Internet at <http://pubs.acs.org>.

Accession Codes

† PDB codes for compounds **5** and **42** are 3SDG and 3SFI, respectively.

■ AUTHOR INFORMATION

Corresponding Author

*Phone: +33 (0)320 964 947. Fax: +33 (0) 320 964 709. E-mail: benoit.deprez@univ-lille2.fr. Home pages: U761, <http://www.deprezlab.fr>; PRIM, <http://www.drugdiscoverylille.org>.

Present Address

† Galapagos N.V., General De Wittelaan L11 A3, 2800, Mechelen, Belgium.

Author Contributions

‡ These authors contributed equally to this work.

■ ACKNOWLEDGMENTS

We thank Eve Willery, Julie Dumont, Youssef Jallouli, and Anne-Sophie Druchbert for technical assistance and Pierre-Marie Danzé and Pr. André Tartar for scientific discussions. We are grateful to the institutions that support our laboratories (Inserm, INSERM-Avenir fellowship to P.B., Institut Pasteur Korea (Grants K204EA000001-08E0100-00100 and K204EA000001-09E0100-00100), Université Lille Nord de France, Institut Pasteur de Lille, CNRS, EU, Région Nord-Pas de Calais, FEDER (Grants 09220019 and 09220020 PRESAGE 31510), ANR (Grant ANR-06-EMPB-033), PRIM (Pôle de Recherche Interdisciplinaire du Médicament), and the European Commission under the 7th

Framework Program (Research Infrastructures (Grant 226716)). Diffraction data were collected at the Swiss Light Source (Paul Scherrer Institute, Villigen, Switzerland). We are grateful to the machine and beamline scientists whose outstanding efforts have made these experiments possible. Data management was performed using Pipeline Pilot from Accelrys. B.V. is a recipient of a doctoral fellowship MENR. We thank Varian Inc. for their technical support. NMR acquisitions were done by the LARMN, Lille, France, and SPR acquisitions were done at the molecular interaction platform (IMPRT-IFR114).

■ ABBREVIATIONS USED

ACM, automated confocal microscopy; AcOEt, ethyl acetate; AcOH, acetic acid; Boc, *tert*-butoxycarbonyl; CH_3CN , acetonitrile; DCM, dichloromethane; DIEA, diisopropylethylamine; DMF, dimethylformamide; DMSO, dimethylsulfoxide; DOTS, directly observed treatment short-course; EDCI, *N*-ethyl-3-(3-dimethylaminopropyl)carbodiimide; ETH, ethionamide; Et_3N , triethylamine; EtOH, ethanol; GFP, green fluorescent protein; HBTU, *O*-benzotriazole-*N,N,N,N*-tetramethyluronium hexafluorophosphate; HOBt, *N*-hydroxybenzotriazole; MDR-TB, multidrug resistant tuberculosis; MeOH, methanol; MIC, minimal inhibitory concentration; PBS, phosphate buffered saline; PK, pharmacokinetic; RT, room temperature; SAR, structure–activity relationship; SPR, surface plasmon resonance; TB, tuberculosis; TEA, triethylamine; THF, tetrahydrofuran; XDR-TB, extensively drug resistant tuberculosis

■ REFERENCES

- (1) World Health Organization. *Global Tuberculosis Control*; World Health Organization: Geneva, 2010; ISBN 978 92 4 156406 9.
- (2) Cox, H. S.; Ford, N.; Reeder, J. C. Are we really that good at treating tuberculosis? *Lancet Infect. Dis.* **2009**, *9*, 138–139.
- (3) Kaufmann, S. H. E. How can immunology contribute to the control of tuberculosis? *Nat. Rev. Immunol.* **2001**, *1*, 20–30.
- (4) Harries, A. D. Tuberculosis and human immunodeficiency virus infection in developing countries. *Lancet* **1990**, *335*, 387–390.
- (5) Koenig, R. Drug-resistant tuberculosis: in South Africa, XDR TB and HIV prove a deadly combination. *Science* **2008**, *319*, 894–897.
- (6) Furin, J. The clinical management of drug-resistant tuberculosis. *Curr. Opin. Pulm. Med.* **2007**, *13*, 212–217.
- (7) Cox, H.; Kebede, Y.; Allamuratova, S.; Ismailov, G.; Davletmuratova, Z.; Byrnes, G.; Stone, C.; Niemann, S.; Rüscher-Gerdes, S.; Blok, L.; Doshetov, D. Tuberculosis recurrence and mortality after successful treatment: impact of drug resistance. *PLoS Med.* **2006**, *3*, 1836–1843.
- (8) Koul, A.; Arnoult, E.; Lounis, N.; Guillemont, J.; Andries, K. The challenge of new drug discovery for tuberculosis. *Nature* **2011**, *469*, 483–490.
- (9) Mitnick, C. D.; McGee, B.; Peloquin, C. A. Tuberculosis pharmacotherapy: strategies to optimize patient care. *Expert Opin. Pharmacother.* **2009**, *10*, 381–401.
- (10) Ejim, L.; Farha, M. A.; Falconer, S. B.; Wildenhain, J.; Coombes, B. K.; Tyers, M.; Brown, E. D.; Wright, G. D. Combinations of antibiotics and nonantibiotic drugs enhance antimicrobial efficacy. *Nat. Chem. Biol.* **2011**, *7*, 348–350.
- (11) Lounis, N.; Veziris, N.; Chauffour, A.; Truffot-Pernot, C.; Andries, K.; Jarlier, V. Combinations of R207910 with drugs used to treat multidrug-resistant tuberculosis have the potential to shorten treatment duration. *Antimicrob. Agents Chemother.* **2006**, *50*, 3543–3547.
- (12) Cox, H.; Kebede, Y.; Allamuratova, S.; Ismailov, G.; Davletmuratova, Z.; Byrnes, G.; Stone, C.; Niemann, S.; Rüscher-Gerdes, S.; Blok, L.; Doshetov, D. Tuberculosis recurrence and mortality after successful treatment: impact of drug resistance. *PLoS Med.* **2006**, *3*, e384.
- (13) DeBarber, A. E.; Mdluli, K.; Bosman, M.; Bekker, L. G.; Barry, C. E. Ethionamide activation and sensitivity in multidrug-resistant

Mycobacterium tuberculosis. *Proc. Natl. Acad. Sci. U.S.A.* **2000**, *97*, 9677–9682.

(14) Baulard, A. R.; Betts, J. C.; Engohang-Ndong, J.; Quan, S.; McAdam, R. A.; Brennan, P. J.; Loch, C.; Besra, G. S. Activation of the pro-drug ethionamide is regulated in *Mycobacteria*. *J. Biol. Chem.* **2000**, *275*, 28326–28331.

(15) Willand, N.; Dirie, B.; Carette, X.; Bifani, P.; Singhal, A.; Desroses, M.; Leroux, F.; Willery, E.; Mathys, V.; Deprez-Poulain, R.; Delcroix, G.; Frenois, F.; Aumercier, M.; Loch, C.; Villeret, V.; Deprez, B.; Baulard, A. R. Synthetic EthR inhibitors boost antituberculous activity of ethionamide. *Nat. Med.* **2009**, *15*, 537–544.

(16) Flipo, M.; Desroses, M.; Lecat-Guillet, N.; Dirie, B.; Carette, X.; Leroux, F.; Piveteau, C.; Demirkaya, F.; Lens, Z.; Rucktooa, P.; Villeret, V.; Christophe, T.; Jeon, H. K.; Loch, C.; Brodin, P.; Deprez, B.; Baulard, A. R.; Willand, N. Ethionamide boosters: synthesis, biological activity, and structure–activity relationships of a series of 1,2,4-oxadiazole EthR inhibitors. *J. Med. Chem.* **2011**, *54*, 2994–3010.

(17) Christophe, T.; Jackson, M.; Jeon, H. K.; Fenistein, D.; Contreras-Dominguez, M.; Kim, J.; Genovesio, A.; Carralot, J.-P.; Ewann, F.; Kim, E. H.; Lee, S. Y.; Kang, S.; Seo, M. J.; Park, E. J.; Skovierova, H., H.; Pham, H.; Riccardi, G.; Nam, J. Y.; Marsollier, L.; Kempf, M.; Joly-Guillou, M.-L.; Oh, T.; Shin, W. K.; No, Z.; Nehrbass, U.; Brosch, R.; Cole, S. T.; Brodin, P. High content screening identifies decaprenyl-phosphoribose 2' epimerase as a target for intracellular antimycobacterial inhibitors. *PLoS Pathog.* **2009**, *5*, e1000645.

(18) Christophe, T.; Ewann, F.; Jeon, H. K.; Cechetto, J.; Brodin, P. High-content imaging of *Mycobacterium tuberculosis*-infected macrophages: an in vitro model for tuberculosis drug discovery. *Future Med. Chem.* **2010**, *2*, 1283–1293.

(19) Engohang-Ndong, J.; Baillat, D.; Aumercier, M.; Bellefontaine, F.; Besra, G. S.; Loch, C.; Baulard, A. R. EthR, a repressor of the TetR/CamR family implicated in ethionamide resistance in mycobacteria, octamerizes cooperatively on its operator. *Mol. Microbiol.* **2004**, *51*, 175–188.

(20) Mega, J. L.; Close, S. L.; Wiviott, S. D.; Shen, L.; Hockett, R. D.; Brandt, J. T.; Walker, J. R.; Antman, E. M.; Macias, W. L.; Braunwald, E.; Sabatine, M. S. Cytochrome P450 genetic polymorphisms and the response to prasugrel: relationship to pharmacokinetic, pharmacodynamic, and clinical outcomes. *Circulation* **2009**, *119*, 2553–2560.

(21) Mosier, P. D.; Jurs, P. C.; Custer, L. L.; Durham, S. K.; Pearl, G. M. Predicting the genotoxicity of thiophene derivatives from molecular structure. *Chem. Res. Toxicol.* **2003**, *16*, 721–732.

(22) Lopez Garcia, M. P.; Dansette, P. M.; Valadon, P.; Amar, C.; Beaune, P. H.; Guengerich, F. P.; Mansuy, D. Human-liver cytochromes P-450 expressed in yeast as tools for reactive-metabolite formation studies. *Eur. J. Biochem.* **1993**, *213*, 223–232.

(23) Khanna, I. K.; Yu, Y.; Huff, R. M.; Weier, R. M.; Xu, X.; Koszyk, F. J.; Collins, P. W.; Cogburn, J. N.; Isakson, P. C.; Koboldt, C. M.; Masferrer, J. L.; Perkins, W. E.; Seibert, K.; Veenhuizen, A. W.; Yuan, J.; Yang, D.-C.; Zhang, Y. Y. Selective cyclooxygenase-2 inhibitors: heteroaryl modified 1,2-diarylimidazoles are potent, orally active antiinflammatory agents. *J. Med. Chem.* **2000**, *43*, 3168–3185.

(24) Poulain, R. F.; Tartar, A. L.; Deprez, B. P. Parallel synthesis of 1,2,4-oxadiazoles from carboxylic acids using an improved, uronium-based, activation. *Tetrahedron Lett.* **2001**, *42*, 1495–1498.

(25) Braisted, A. C.; Oslob, J. D.; Delano, W. L.; Hyde, J.; McDowell, R. S.; Waal, N.; Yu, C.; Arkin, M. R.; Raimundo, B. C. Discovery of a potent small molecule IL-2 inhibitor through fragment assembly. *J. Am. Chem. Soc.* **2003**, *125*, 3714–3715.

(26) Lipinski, C. A.; Lombardo, F.; Dominy, B. W.; Feeney, P. J. Experimental and computational approaches to estimate solubility and permeability in drug discovery and development settings. *Adv. Drug Delivery Rev.* **2001**, *46*, 3–26.

(27) Veber, D. F.; Johnson, S. R.; Cheng, H. Y.; Smith, B. R.; Ward, K. W.; Kopple, K. D. Molecular properties that influence the oral bioavailability of drug candidates. *J. Med. Chem.* **2002**, *45*, 2615–2623.

(28) Dover, L. G.; Corsino, P. E.; Daniels, I. R.; Cocklin, S. L.; Tatituri, V.; Besra, G. S.; Futterer, K. Crystal structure of the TetR/

CamR family repressor *Mycobacterium tuberculosis* EthR implicated in ethionamide resistance. *J. Mol. Biol.* **2004**, *340*, 1095–1105.

(29) Leslie, A. The integration of macromolecular diffraction data. *Acta Crystallogr., Sect. D: Biol. Crystallogr.* **2006**, *62*, 48–57.

(30) Collaborative Computational Project Number 4. The CCP4 suite: programs for protein crystallography. *Acta Crystallogr., Sect. D: Biol. Crystallogr.* **1994**, *50*, 760–763.

(31) Emsley, P.; Lohkamp, B.; Scott, W. G.; Cowtan, K. Features and development of Coot. *Acta Crystallogr., Sect. D: Biol. Crystallogr.* **2010**, *66*, 486–501.